LEVEL

DTIC
S ELECT
JUN 1 1 1981

C

ULTRASONIC DETERMINATION OF COMBINATIONS OF THIRD-ORDER ELASTIC CONSTANTS OF SMALL CUBIC SINGLE CRYSTALS

BRUCE DION BLACKBURN

M. A. BREAZEALE
PRINCIPAL INVESTIGATOR
ULTRASONICS LABORATORY
DEPARTMENT OF PHYSICS

THE UNIVERSITY OF TENNESSEE
Knoxville, Tennessee

May 1981

Distribution of This Document is Unlimited

81 6 11 060

REPORT DOCUMENTATION PAGE		READ INSTRUCTIONS BEFORE COMPLETING FORM
1. REPORT NUMBER Technical Report 20	2. GOVT ACCESSION NO. AD-A100 038	3. RECIPIENT'S CATALOG NUMBER
4. TITLE *(and Subtitle)* ULTRASONIC DETERMINATION OF COMBINATIONS OF THIRD-ORDER ELASTIC CONSTANTS OF SMALL CUBIC SINGLE CRYSTALS		5. TYPE OF REPORT & PERIOD COVERED Interim
		6. PERFORMING ORG. REPORT NUMBER
7. AUTHOR(s) Bruce Dion Blackburn		8. CONTRACT OR GRANT NUMBER(s) N00014-76-C-0177
9. PERFORMING ORGANIZATION NAME AND ADDRESS Dept. of Physics The University of Tennessee Knoxville, TN 37916		10. PROGRAM ELEMENT, PROJECT, TASK AREA & WORK UNIT NUMBERS
11. CONTROLLING OFFICE NAME AND ADDRESS Office of Naval Research, Code 421 Department of the Navy Arlington, VA 22217		12. REPORT DATE May 1981
		13. NUMBER OF PAGES 97
14. MONITORING AGENCY NAME & ADDRESS*(if different from Controlling Office)*		15. SECURITY CLASS. *(of this report)* Unclassified
		15a. DECLASSIFICATION/DOWNGRADING SCHEDULE

16. DISTRIBUTION STATEMENT *(of this Report)*

Approved for public release; distribution unlimited.

DTIC
ELECT
JUN 11 1981
S
C

17. DISTRIBUTION STATEMENT *(of the abstract entered in Block 20, if different from Report)*

18. SUPPLEMENTARY NOTES

19. KEY WORDS *(Continue on reverse side if necessary and identify by block number)*

Third-order elastic constants	Harmonic generation
Nonlinearity parameter	Capacitive detector
Diffraction of a finite amplitude wave	Cubic crystals
Cesium cadmium fluoride	Ultrasonic wave propagation
Potassium zinc fluoride	Nonlinear acoustics

20. ABSTRACT *(Continue on reverse side if necessary and identify by block number)*
The ultrasonic harmonic generation technique for measuring combinations of third-order elastic constants of cubic single crystals previously has been limited by the plane wave approximation to measurement of samples whose cross sectional dimensions are $\gtrsim$ 1.5 cm. By obtaining data with small transducers and considering the effects of diffraction, the range of samples measurable with the technique has been extended to samples of $\sim$ 5 mm on a side. This development has made possible measurement of single crystals unavailable in larger dimensions. The minimum length required for measurement depends on

DD FORM 1473 EDITION OF 1 NOV 65 IS OBSOLETE
1 JAN 73
S/N 0102-LF-014-6601

20. (continued)

the material and on the cross sectional dimensions; the current e? ?te of
the minimum length is ~ 4 mm. Diffraction corrections based on tn? ?rchhoff
diffraction theory are presented and analyzed for both the fundame?? ?l fre-
quency component and the second harmonic component of the ultrason? wave.
The technique was used to measure combinations of third-order elast?c constants
of small samples of $CsCdF_3$ and $KZnF_3$. The measured combinations, ?? ?nits of
10^{12} dyn/cm , obtained by correcting only the fundamental frequenc? ?mponent
for diffraction, are ~~as~~ follows.·

Sample	C_{111}	$(C_{112} + 4C_{166})$	$(6C_{144} + C_?$ $- 8C_{456})$
CsCdF$_3$	-13.4	- 7.24	-4?
KZnF$_3$	-16.8	-11.3	

ULTRASONIC DETERMINATION OF COMBINATIONS OF THIRD-ORDER

ELASTIC CONSTANTS OF SMALL CUBIC SINGLE CRYSTALS

by

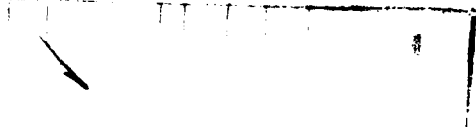Bruce Dion Blackburn

TECHNICAL REPORT NO. 20

Ultrasonics Laboratory
Department of Physics
The University of Tennessee   37916

May 1981

PREFACE

This report is an adaptation of the dissertation of Bruce Dion Blackburn submitted to the Department of Physics at The University of Tennessee in partial fulfillment of the requirements of the degree of Doctor of Philosophy.

The ultrasonic harmonic generation technique for measuring combinations of third-order elastic constants of cubic single crystals previously has been limited by the plane wave approximation to measurement of samples whose cross sectional dimensions are $\gtrsim$ 1.5 cm. By obtaining data with small transducers and considering the effects of diffraction, the range of samples measurable with the technique has been extended to samples of 5 mm on a side. This development has made possible measurement of single crystals unavailable in larger dimensions. The minimum length required for measurement depends on the material and on the cross sectional dimensions; the current estimate of the minimum length is 4 mm. Diffraction corrections based on the Kirchhoff diffraction theory are presented and analyzed for both the fundamental frequency component and the second harmonic component of the ultrasonic wave. The technique was used to measure combinations of third-order elastic constants of small samples of $CsCdF_3$ and $KZnF_3$.

The author expresses his sincere appreciation to Professor M. A. Breazeale for his suggestion of the topic and guidance during the research. He is grateful to Dr. W. T. Yost for his help in familiarizing him with the experimental procedure. Thanks are extended to Professor A. Zarembowitch of the Université Pierre et Marie Curie, Paris, France, for loaning the $CsCdF_3$ and $KZnF_3$ samples, and to Mr. D. W. Fitting for

providing the computer program for $\{D_L\}$. He would like to thank Mrs. Maxine Martin for typing the manuscript.

TABLE OF CONTENTS

LIST OF TABLES

LIST OF FIGURES

CHAPTER I

INTRODUCTION

The general objective of the research described here is to measure combinations of third-order elastic constants of cubic single crystals. In the macroscopic theory of elasticity, the strain energy density of the crystal can be expressed as a power series expansion in terms of the elements of the strain tensor. The coefficients of the second-order terms, multiplied by (2!), are called second-order elastic constants; the third-order elastic constants are the coefficients of the third-order terms, multiplied by (3!).

In the microscopic theory, the potential energy of the crystal can be expressed as a Taylor series in terms of the displacements of the atoms from their equilibrium positions. The coefficients in this series are called coupling parameters.

Pfleiderer (1962) and Coldwell-Horsfall (1963) expressed the second- and third-order coupling parameters for face-centered cubic crystals in terms of the second- and third-order elastic constants, assuming nearest neighbor interactions only. Coldwell-Horsfall (1963) presented similar relations for body-centered cubic crystals, assuming nearest and next-nearest neighbor interactions, and examined the case of central forces for both lattice types. Measurements of third-order elastic constants can therefore give information about the interatomic potential and forces between atoms.

1

Several physical properties of solids result from, or depend upon, the presence of the anharmonic terms in the strain energy density. These properties include thermal expansion, heat conduction, the proportionality of specific heat to temperature at temperatures above the characteristic Debye temperature, the difference between isothermal and adiabatic elastic constants, the dependence of second-order elastic constants on temperature and pressure, the interaction of two lattice waves, the attenuation of high frequency sound waves, and waveform distortion of sound waves.

Several experimental techniques have been used to measure third-order elastic constants of various solids. Measurement of the dependence of the second-order elastic constants on hydrostatic pressure gives combinations of third-order elastic constants but does not give the complete set of these constants for a particular crystal structure. Lazarus (1949) measured the pressure dependence of the second-order elastic constants of single crystals of NaCl, KCl, CuZn, Cu, and Al. Daniels and Smith (1958) made similar measurements on Cu, Ag, and Au. Hearmon (1953), using equations obtained by Birch (1947), determined what combinations of third-order elastic constants could be calculated from Lazarus' data.

Seeger and Buck (1960) and Melngailis, Maradudin, and Seeger (1963) proposed an optical method of measuring third-order elastic constants of transparent crystals, and Parker, Kelly, and Bolef (1964) used the method to measure a third-order elastic constant (C_{111}) of NaCl. An initially sinusoidal finite amplitude ultrasonic wave propagating through the crystal distorts as it propagates, producing an asymmetric diffraction pattern of monochromatic light directed perpendicular to the

direction of the sound wave. Combinations of third-order elastic constants can be calculated from measurements of the light intensities in the positive and negative diffraction orders.

Barker and Hollenbach (1970) developed an interesting technique for measuring third- and higher-order elastic constants. The sample is struck by a projectile (and destroyed), and the resulting strain is measured. Graham (1972) calculated elastic constants of fused silica and sapphire from the data of Barker and Hollenbach (1970) and Graham and Brooks (1971).

One of the most widely used methods of measuring third-order elastic constants requires a measurement of the change in sound velocity with uniaxial stress. The first determination of a complete set of third-order elastic constants of isotropic materials was made by Hughes and Kelly (1953) by measuring the change of ultrasonic velocity with hydrostatic pressure and with uniaxial stress in poly-styrene, iron, and pyrex glass. For the case of cubic crystals, Seeger and Buck (1960) obtained relations for the sound velocities in crystals subjected to hydrostatic pressure and uniaxial stress, in terms of second- and third-order elastic constants. Bateman, Mason, and McSkimin (1961) then performed the measurements on the cubic crystal germanium and obtained the first complete set of six third-order elastic constants of a cubic crystal. Measurements followed by Drabble and Gluyas (1963) on germanium, McSkimin and Andreatch (1964) on germanium and silicon, Bogardus (1965) on germanium, magnesium oxide, and fused silica, Chang (1965) on NaCl and KCl, and Thurston, McSkimin, and Andreatch (1966) on quartz. The third-order elastic constants obtained

by this method are neither truly adiabatic nor isothermal because an adiabatic wave propagates through an isothermally stressed medium (Skove and Powell, 1967).

To apply the above technique to metals would require small stresses because metal single crystals are easily deformed plastically. Hiki and Granato (1966) used a sensitive method of measuring changes in velocity with stress to measure complete sets of six third-order elastic constants of prestressed single crystals of copper, silver, and gold.

Another approach to the determination of third-order elastic constants involves the nonlinear phenomenon of the interaction of elastic waves. Jones and Kobett (1963) performed classical calculations of the scattering of two plane, intersecting, elastic waves in an anisotropic medium. Their predicted scattered waves were experimentally detected by Rollins (1963). Taylor and Rollins (1964) presented a quantum mechanical treatment of the process, and their results were compared with experimental measurements by Rollins, Taylor, and Todd (1964). Dunham and Huntington (1970) extended the theory of Taylor and Rollins and performed an experimental study using samples of fused silica and NaCl.

In the present experiments, combinations of third-order elastic constants are measured by an ultrasonic harmonic generation technique. As an initially sinusoidal wave propagates through a solid, higher harmonics are generated. This effect was observed and first reported by Gedroits and Krasilnikov (1963) and Breazeale and Thompson (1963). Breazeale and Ford (1965) established a relationship between the

third-order elastic constants and the solution to the nonlinear equation describing the propagation of an initially sinusoidal ultrasonic wave along a pure longitudinal mode direction in a cubic crystal. By measuring the amplitudes of the fundamental and second harmonic components, certain combinations of third-order elastic constants can be calculated, as described in Chapter II. A capacitive receiver capable of measuring the absolute amplitudes of the fundamental and second harmonic components of a plane wave was developed by Gauster and Breazeale (1966), and they used the receiver to measure combinations of third-order elastic constants of copper. Yost and Breazeale (1973) then used the capacitive receiver for measurements on fused silica and combined their results with the results of Dunham and Huntington (1970) to obtain the first complete set of adiabatic third-order elastic constants.

The harmonic generation technique has been valuable for low temperature measurements. Meeks and Arnold (1970) used the technique to measure combinations of third-order elastic constants of strontium titanate between 106 and 300°K, after Mackey and Arnold (1969) had performed the measurements at room temperature. Peters, Breazeale, and Paré (1968) developed a pneumatically controlled variable gap capacitive receiver to be used for low temperature measurements, and they used it to measure combinations of third-order elastic constants of copper down to liquid nitrogen temperature (Peters, Breazeale, and Paré, 1970). Similar measurements were performed on germanium (Yost and Breazeale, 1974). Bains and Breazeale (1976) then extended the technique through liquid helium temperature and measured germanium, and temperature

dependent measurements followed on four types of fused silica (Cantrell and Breazeale, 1978), on copper (Yost, Cantrell, and Breazeale, 1980), and on silicon (Philip and Breazeale, 1981).

In previous experiments, the measurements were performed on single crystals that were large enough to allow the use of transducers whose diameter to wavelength ratio permitted a plane wave approximation. However, some single crystal samples are not available in large sizes. To perform the measurements on smaller samples would require smaller diameter transducers. With a smaller diameter to wavelength ratio the plane wave approximation might no longer be valid and diffraction effects would need to be considered. The objectives of the present research were to develop the capability to perform the measurements on small samples, to present a theoretical model consistent with the results, and to use the method to make the measurements on a small sample.

A theory treating the generation of the second harmonic component in the field of a plane circular piston radiating into a fluid has been presented by Ingenito and Williams (1971). They solved a nonlinear wave equation by means of first-order perturbation theory to obtain an expression for the second harmonic as a function of position, in terms of an integral of the square of the fundamental component. They presented an expression for the value of the second harmonic integrated over a circular area coaxial with the source and of the same diameter as the source, and an expression for the second harmonic on the axis. Rogers (1970) presented a theory on the same topic. Kunitsyn and Rudenko (1978) treated the problem by solving the nonlinear equation

describing diffraction in the quasioptical approximation using the method of successive approximations. Lockwood, Muir, and Blackstock (1973) approached the problem by using weak-shock theory and restricted their analysis to the far (Fraunhofer) field.

In the present experiments, in order to develop the capability to perform the measurements on small samples, data were initially taken on large samples of copper. Combinations of third-order elastic constants of copper had been previously measured in the same laboratory by the harmonic generation technique, allowing an opportunity for comparison of the results of the present experiments with previous results. The small samples on which measurements were made were two members of the perovskite family, $CsCdF_3$ and $KZnF_3$. Professor A. Zarembowitch and others at the Université Pierre et Marie Curie, Paris, France, have been studying structural phase transitions between the cubic and tetragonal structure in fluoperovskites and attempting to establish a connection between these instabilities and the nonlinear behavior of the materials. The data obtained in the present experiments complement their data, which is reported by Fischer (1979) and Fischer, Zarembowitch, and Breazeale (1981).

CHAPTER II

THEORY OF ULTRASONIC NONLINEARITY IN SOLIDS

The theory of ultrasonic nonlinearity in solids can be treated using classical continuum mechanics or quantum mechanics. A treatment using continuum mechanics will be presented in this chapter. The quantum mechanical approach gives identical results [cf. the tutorial paper by Bajak and Breazeale (1980)]. In the classical treatment the equations of motion are obtained from Lagrange's equations for continuous media. The potential energy term in the Lagrangian density is the strain energy density which is written in terms of the Lagrangian strains. The resulting equations of motion are simplified and solved. The solution shows that combinations of third-order elastic constants can be obtained by measurement of displacement amplitudes.

I. DEFINITION OF LAGRANGIAN STRAINS

Let the position of a point in an unstrained solid be given by the coordinates (a_1, a_2, a_3). When the solid is strained, let the position of the point be given by the coordinates (x_1, x_2, x_3). The components of the displacement are

$$u_i = x_i - a_i .$$

(II.1)

The subscript i can have the value 1, 2, or 3.

The square of the distance between two points that are close together is

$$d\ell^2 = da_i^2 \, , \qquad\qquad\qquad\qquad (II.2)$$

using the Einstein summation convention of summing over repeated indices. The square of the distance between the two points in the strained state is

$$d\ell'^2 = dx_i^2 = (da_i + du_i)^2 = (da_i + \frac{\partial u_i}{\partial a_j} da_j)^2$$

$$= da_i^2 + 2 \frac{\partial u_i}{\partial a_j} da_i da_j + \frac{\partial u_i}{\partial a_j} \frac{\partial u_i}{\partial a_k} da_j da_k \, . \qquad (II.3)$$

Since $d\ell^2 = da_i^2$, the above equation is

$$d\ell'^2 - d\ell^2 = 2[\frac{1}{2} (\frac{\partial u_i}{\partial a_j} + \frac{\partial u_j}{\partial a_i} + \frac{\partial u_k}{\partial a_i} \frac{\partial u_k}{\partial a_j})] da_i da_j$$

$$= 2\eta_{ij} da_i da_j \, . \qquad\qquad\qquad (II.4)$$

The η_{ij} are the elements of the Lagrangian strain tensor.

II. THE EQUATIONS OF MOTION

The equations of motion can be obtained from Lagrange's equations for continuous media (Holt and Ford, 1967). Lagrange's equations are

$$\frac{d}{dt} (\frac{\partial L}{\partial \dot{x}_i}) + \frac{d}{da_k} (\frac{\partial L}{\partial(\partial x_i/\partial a_k)}) = 0 \, . \qquad (II.5)$$

The Lagrangian density is

$$L = \frac{1}{2} \rho \dot{x}_i^2 - \phi(\eta) \, , \qquad \qquad (\text{II.6})$$

where ρ is the unstrained mass density and $\phi(\eta)$ is the strain energy per unit unstrained volume. The properties of the medium enter the equations of motion through the strain energy density $\phi(\eta)$.

III. THE ELASTIC CONSTANTS

The strain energy density can be written as a power series expansion about the state of zero strain in terms of the Lagrangian strains:

$$\phi(\eta) = \phi_0 + \phi_1 + \phi_2 + \phi_3 + \dots \, . \qquad \qquad (\text{II.7})$$

The first term, ϕ_0, represents the energy of the unstrained medium and is constant; the second term, ϕ_1, is zero because the first derivative of ϕ with respect to strain, evaluated at zero strain, is equal to zero. The terms of order higher than three are neglected. The terms that will be of interest in Lagrange's equations can be written, using the Einstein summation convention,

$$\phi_2 = \frac{1}{2!} C_{ijk\ell} \eta_{ij} \eta_{k\ell} \, , \qquad \qquad (\text{II.8})$$

and

$$\phi_3 = \frac{1}{3!} C_{ijk\ell mn} \eta_{ij} \eta_{k\ell} \eta_{mn} \, . \qquad \qquad (\text{II.9})$$

The coefficients $C_{ijk\ell}$ appearing in the second-order terms are called

the second-order elastic constants and the $C_{ijk\ell mn}$ are called the
third-order elastic constants.

The elastic constants can also be defined with a thermodynamic
approach if the physical process being considered is purely adiabatic
or purely isothermal. Denoting the internal energy per unit volume
by U and the Helmholtz free energy per unit volume by F, the elastic
constants are defined (Brugger, 1964) by

$$C_{ijk\ell\,\ldots}^{S} = \left\{ \frac{\partial^{n}U}{\partial^{n}\eta_{ij}\,\partial^{n}\eta_{k\ell}\,\cdots} \right\}_{S} \qquad \text{(adiabatic, } n \geq 2\text{)} \qquad \text{(II.10)}$$

and

$$C_{ijk\ell\,\ldots}^{T} = \left\{ \frac{\partial^{n}F}{\partial^{n}\eta_{ij}\,\partial^{n}\eta_{k\ell}\,\cdots} \right\}_{T} \qquad \text{(isothermal, } n \geq 2\text{)} , \qquad \text{(II.11)}$$

where S denotes the entropy and T denotes the temperature.

The elastic constants defined by Eq. (II.10) are called adiabatic
elastic constants, and the elastic constants defined by Eq. (II.11) are
called isothermal elastic constants. Since F = U - TS, the distinction
does not apply at absolute zero.

The propagation of an ultrasonic wave through an unstrained
medium is an adiabatic process. To describe this process, the strain
energy density ϕ appearing in the Lagrangian density is identified with
the internal energy density U. Thus, the quantities measured in the
present experiments are combinations of adiabatic third-order elastic
constants.

In general there are 81 second-order and 729 third-order elastic constants. The number of independent constants is lower if there are lattice symmetries. For all cubic crystals there are three independent second-order elastic constants, and for the most symmetrical classes of cubic crystals there are six independent third-order elastic constants (Birch, 1947). All of the samples measured in the present experiments were cubic crystals having six independent third-order elastic constants.

It is conventional and convenient to contract the subscript notation for the elastic constants (Voigt, 1928) as follows:

$$11 \rightarrow 1, \ 22 \rightarrow 2, \ 33 \rightarrow 3, \ 23 \rightarrow 4, \ 13 \rightarrow 5, \ 12 \rightarrow 6 \ .$$

Since the strain tensor elements η_{ij} are symmetric, permutations of the subscripts ij are equivalent. The subscript notation for the strains will not be contracted. Using Brugger's (1964) notation, the three independent second-order elastic constants for cubic crystals are C_{11}, C_{12}, and C_{44}, and the six independent third-order elastic constants are C_{111}, C_{112}, C_{123}, C_{144}, C_{166}, and C_{456}.

IV. THE NONLINEAR WAVE EQUATION AND ITS SOLUTION

The nonlinear wave equation describing the propagation of an ultrasonic wave through the sample can be obtained from Lagrange's equations (II.5). Identifying $\Phi(\eta)$, appearing in the Lagrangian density (II.6), with the internal energy per unit volume U, as previously discussed, the following equation can be obtained:

$$\rho \ddot{x}_i = \frac{d}{da_k} \left[\frac{\partial U}{\partial n_{ik}} + \frac{\partial U}{\partial n_{qk}} \frac{\partial u_i}{\partial a_q} \right] .$$

(II.12)

This equation applies for any direction of propagation and any wave polarization. It can be simplified by considering only pure mode longitudinal plane waves. Pure longitudinal waves can propagate in the [100], [110], and [111] directions in a cubic crystal. The equation of motion pertaining to a pure longitudinal plane wave propagating in one of these three directions becomes (Breazeale and Ford, 1965)

$$\rho \ddot{u} = K_2 \frac{\partial^2 u}{\partial a^2} + (3K_2 + K_3) \frac{\partial u}{\partial a} \frac{\partial^2 u}{\partial a^2} ,$$

(II.13)

where K_2 and K_3 are linearly independent combinations of second-order and third-order elastic constants, respectively, as shown in Table II-1.

The perturbation solution (valid for distances much less than the discontinuity distance) to Eq. (II.13) is given by Breazeale and Ford (1965) for a sinusoidal driver located at a = 0 by

$$u = A_1 \sin(ka - \omega t) - (\frac{3K_2 + K_3}{8K_2})A_1^2 k^2 a \cos 2(ka - \omega t) + \dots ,$$

(II.14)

where

A_1 is the displacement amplitude of the fundamental frequency component at a = 0,

k is the wavenumber,

a is the distance of propagation,

ω is the angular frequency,

t is time.

Table II-1. K_2 and K_3 for the Principal Directions in a Cubic Crystal

Direction	K_2	K_3
[100]	C_{11}	C_{111}
[110]	$\dfrac{C_{11} + C_{12} + 2C_{44}}{2}$	$\dfrac{C_{111} + 3C_{112} + 12C_{166}}{4}$
[111]	$\dfrac{C_{11} + 2C_{12} + 4C_{44}}{3}$	$\frac{1}{9}\,(C_{111} + 6C_{112} + 12C_{144} + 24C_{166} + 2C_{123} + 16C_{456})$

The first term in the solution is the component having the fundamental frequency; the second term is the component having the second harmonic frequency. The solution also contains higher harmonic terms which have been neglected. The amplitude of the second harmonic component, denoted by A_2, is given by

$$A_2 = -(\frac{3K_2 + K_3}{8K_2})A_1^{2}k^2a ,$$
(II.15)

and is seen to be proportional to the square of the fundamental amplitude, the square of the frequency, the propagation distance, and a term containing the combinations of elastic constants. By measuring the displacement amplitudes of the fundamental and second harmonic components and knowing the value of K_2, the combinations of third-order elastic constants K_3 can be calculated. The value of K_2 for a given direction is given by

$$K_2 = \rho v^2$$
(II.16)

where v is the velocity of sound in the given direction. Rearranging Eq. (II.15) gives

$$K_3 = -K_2(3 + \frac{8A_2}{A_1^{2}k^2a}) = -K_2(3 + \beta) .$$
(II.17)

The second term in the parentheses in Eq. (II.17) is denoted by β:

$$\beta = \frac{8A_2}{A_1^2 k^2 a} = -\left(\frac{3K_2 + K_3}{K_2}\right) . \tag{II.18}$$

The quantity β is equal to the negative of the ratio of the coefficient in the nonlinear term in the wave equation (II.13) to the coefficient in the linear term; β is therefore called the nonlinearity parameter. (This definition of the nonlinearity parameter β is consistent with the corresponding definition for liquids and gases. The expression given for β is a factor of three greater than the expression used for β by Cantrell (1976).)

The theory presented in this chapter has led to an equation that shows that the nonlinearity parameter β (and K_3) can be determined from a measurement of the amplitudes of the first and second harmonic components of a plane wave. Two of the objectives of the present research are to develop the capability to measure these quantities using waves that are not plane, and to form a better understanding of the diffraction of an ultrasonic wave propagating in a nonlinear medium. A comparison of the values to be measured with accepted values of β and K_3 serves as a basis for formulating an approach to nonlinear diffraction theory.

CHAPTER III

APPARATUS, PROCEDURE, AND SAMPLES

I. EXPERIMENTAL CONSIDERATIONS

The method of measuring the displacement amplitudes of the fundamental and second harmonic components of a plane ultrasonic wave propagating through a solid sample will be discussed in this chapter. For the experiments to be described, as well as for previous experiments [Gauster (1966) and others], a fundamental frequency of 30 MHz was selected for the following reasons. The amplitude of the second harmonic component is proportional to the square of the fundamental frequency; therefore the higher the frequency, the better the signal to noise ratio. However, attenuation and the effects of nonparallelism of the surfaces of the sample also increase with increasing frequency. A frequency of 30 MHz was found to be a good compromise. Also, the diameters of the transducers used in previous measurements were large enough (1.27 cm) that the diameter to wavelength ratio using 30 MHz was large enough to justify a plane wave approximation.

The ultrasonic wave was pulsed in order to avoid interference effects. A pulse repetition rate of 60 pulses/second was used to minimize heating of the sample.

In the theory of finite amplitude wave propagation the second harmonic amplitude is related to the fundamental amplitude by a simple integral power law only in the limit of infinitesimal fundamental

17

amplitude (Thurston and Shapiro, 1967). Therefore the initial
fundamental amplitudes were minimized to levels providing useful signal
to noise ratios for the generated second harmonic components.

II. THE DETECTOR APPARATUS

The measurements of the displacement amplitudes were made using
the detector apparatus pictured in Figure III-1. A cross sectional view
of the apparatus is shown in Figure III-2. An ultrasonic pulse is
transmitted into the sample from a piezoelectric x-cut quartz transducer
and causes the optically flat end of the sample to vibrate. An optically
flat electrode is located approximately ten microns below the end of the
sample and forms parallel plate capacitor with it. A dc bias voltage
of the order of 150 volts is applied across this capacitor. When the
ultrasonic pulse impinges upon the end of the sample, the gap spacing
of the capacitor changes, and a current is produced. The fundamental
frequency signal and the second harmonic signal are separated electronically.
The displacement amplitudes A_1 and A_2 are calculated by determining the
current and the initial gap spacing.

The initial gap spacing is measured with an impedance bridge. The
current is determined by measuring the voltage across a known impedance.
Since it is preferable to measure a continuous voltage rather than a pulsed
signal, a substitutional continuous signal is used which is adjusted to
produce the same output signal as that received using the pulsed ultra-
sonic wave.
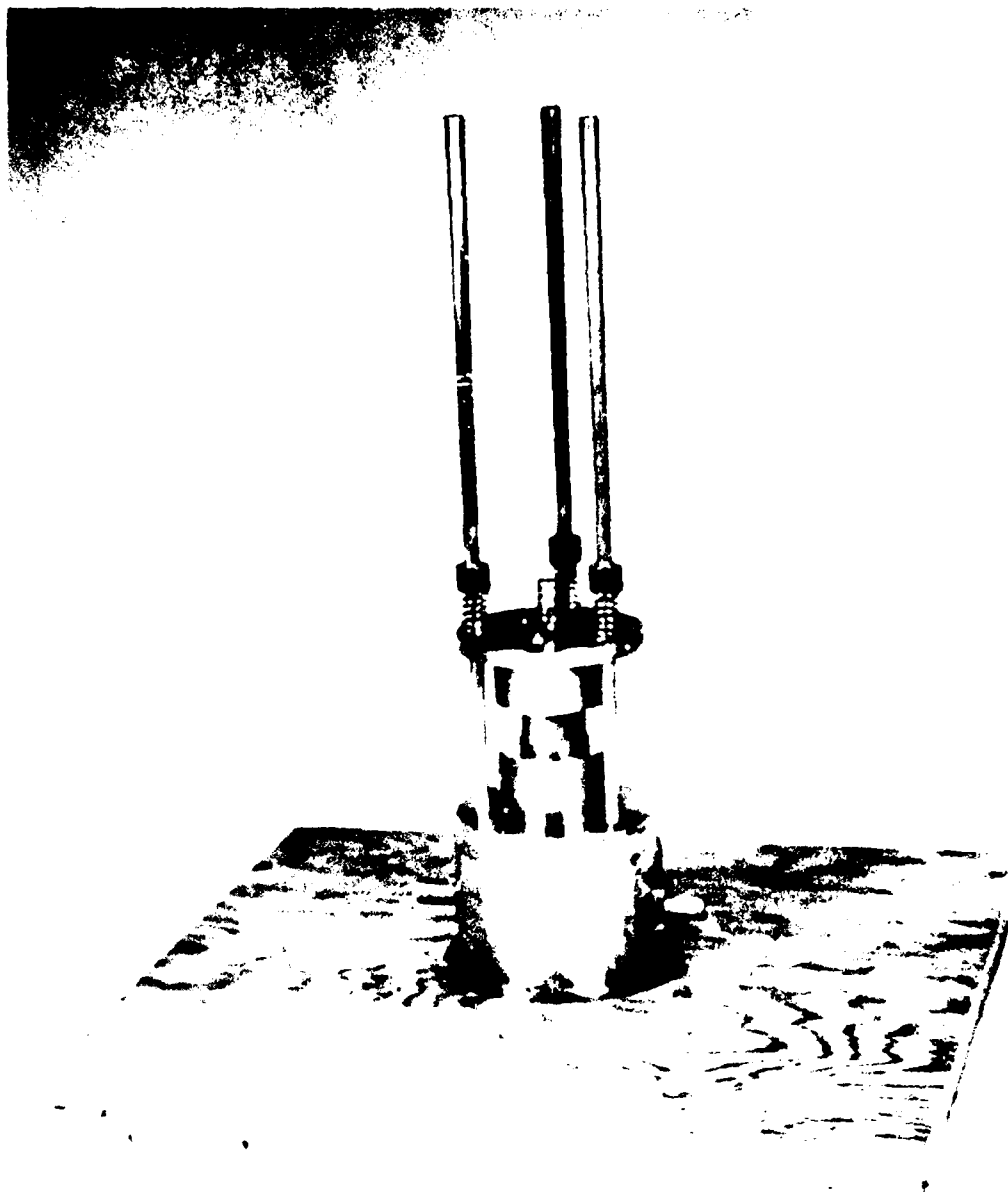
Figure III-1. The detector apparatus. A 2.5 cm diameter sample is shown.
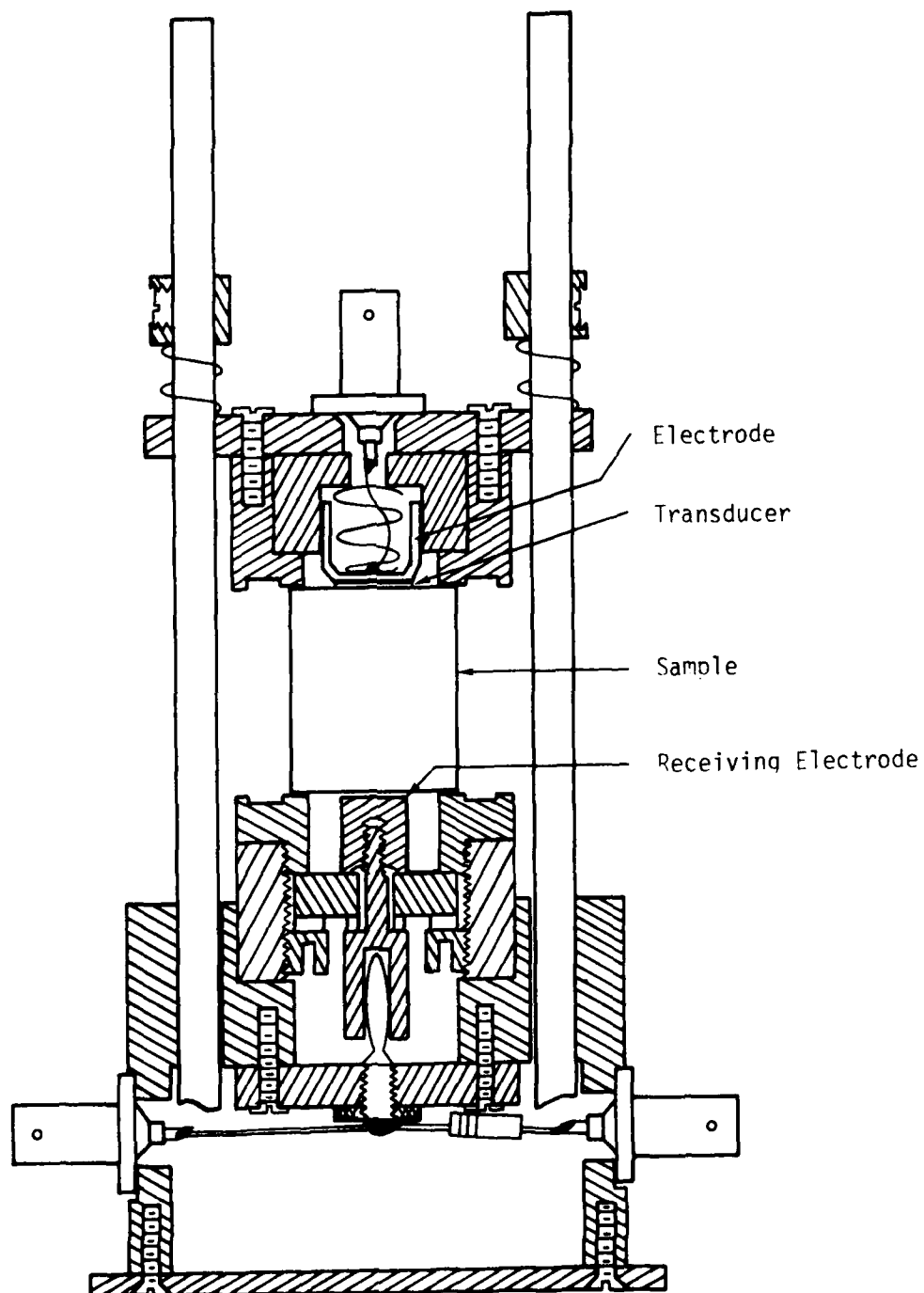
Figure III-2. Cross sectional view of the detector apparatus.

III.   CALIBRATION AND PROCEDURE

The circuit diagram used for calculating the amplitudes is shown in Figure III-3.   The detector circuit is represented by a Norton equivalent circuit.   The circuit elements and parameters are defined as follows.

C_D is the quiescent capacitance of the detector,

C_S is the stray capacitance of the detector,

L is the inductance of the wire leading from the banana jack to the BNC connector (shown in Figure III-2).

Z is the impedance of the resistor located in the base of the apparatus, indicated in Figure III-2,

G_D is the current generator of the Norton equivalent circuit of the detector,

G_S is the substitutional signal current generator,

i_D is the amplitude of the current produced by the ultrasonic wave,

i_S is the amplitude of the substitutional current,

S_1 is a "switch" that is opened and closed by turning on or off the ultrasonic pulse,

S_2 is a "switch" that is opened and closed by disconnecting or connecting a signal generator.

Peters (1968) showed that the Thévenin equivalent circuit of the capacitive receiver is a voltage source of voltage amplitude

$$V = \frac{2AV_b}{S_0} ,$$

(III.1)
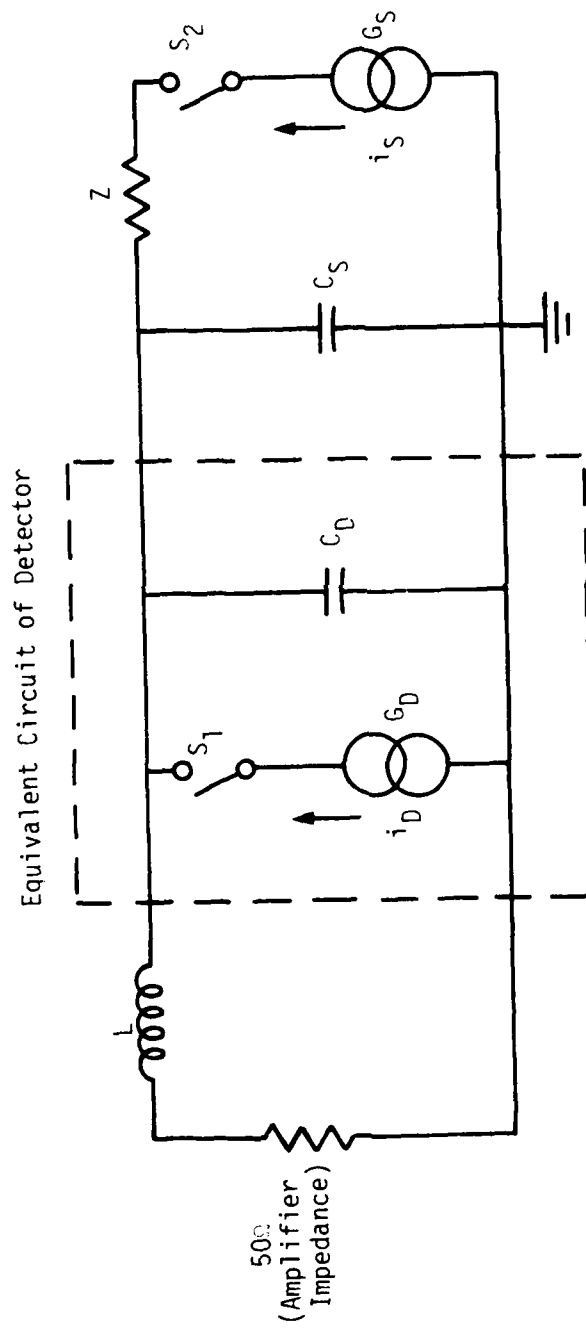
Figure III-3. Equivalent circuit used for the displacement amplitude measurements.

in series with a capacitor C_D, feeding the amplifier impedance. In Eq. (III.1), A is the displacement amplitude of the ultrasonic wave within the solid, V_b is the dc bias voltage applied across the capacitive receiver, and S_0 is the gap spacing of the quiescent capacitive receiver. The amplitude of vibration of the free surface of the sample is twice the amplitude within the sample because the incident and reflected waves add. This was taken into account in obtaining Eq. (III.1).

The current amplitude i_D produced by the capacitive detector is related to the voltage amplitude V by

$$i_D = V\omega C_D ,$$
(III.2)

where ω is the angular frequency of vibration. Combining Eqs. (III.1) and (III.2) gives

$$i_D = \frac{2AV_b\omega C_D}{S_0} .$$
(III.3)

The output from the substitutional source G_S is adjusted to give the same output from the amplifier as the output resulting from the ultra-sonic pulse. Under this condition, i_D is equal to i_S, and the displacement amplitude A can be calculated from Eq. (III.3) by measuring i_S.

The current i_S is determined by measuring the voltage V_S across the current generator G_S and measuring the impedance through which i_S passes. The equation is

$$i_S = \frac{V_S}{|Z + [j\omega(C_D + C_S) + \frac{1}{50 + j\omega L}]^{-1}|} \quad . \tag{III.4}$$

The quantity Z is the impedance of the resistor located between the substitutional source and the capacitive detector. At the frequencies used in these experiments, the impedance of the resistor is not purely resistive and is a function of frequency. The impedance can be determined by the following procedure. Refer to Figure III-4 which shows the circuit used for the measurement of the impedance Z. The sample, detector assembly, and bottom plate are removed from the apparatus, and 50 Ω terminators are connected to the two BNC connectors at the base of the apparatus. A cw variable-frequency signal generator is connected to the terminator on the side having the resistor. Probes A and B of a (Hewlett-Packard 8405A) vector voltmeter are positioned at point 1, the phase angle between the signals is zeroed, and the voltages are measured. Probe B is then moved to point 2, leaving probe A at point 1. The signal generator is adjusted to give the same channel A voltage as before, and the channel B voltage and the phase angle are measured. The impedance Z is calculated from the formula

$$Z = [j\omega C + \frac{1}{R_1 + j\omega L}]^{-1} \frac{V_{B1} - V_{B2}e^{j\phi}}{V_{B2}e^{j\phi}} , \tag{III.5}$$

where C is the stray capacitance at point 2, including the probe tip capacitance, R_1 is the resistance of the precision terminator measured with an impedance bridge, V_{B1} and V_{B2} are the voltages measured by
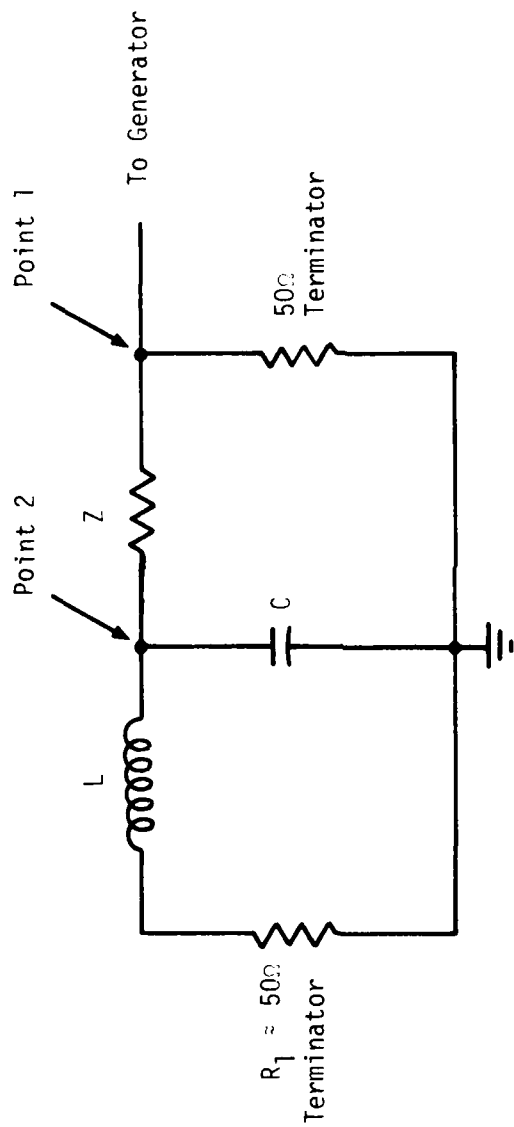
Figure III-4. Circuit used for the measurement of the impedance Z.

probe B at points 1 and 2, respectively, and ϕ is the phase angle. The other symbols were defined previously.

The quantities C, R_1, and L were measured. The value of L was 3.8×10^{-8} H; the value of R_1 for the particular terminator used was 49.74 Ω. The value of the stray capacitance C depends on the configuration during the voltage measurements; in the present measurement C was measured to be 10.75×10^{-12} F. Measurements of the impedance Z were performed at the five frequencies from 28.0 MHz to 32.0 MHz in increments of 1.0 MHz and at the five frequencies from 56.0 MHz to 64.0 MHz in increments of 2.0 MHz. A computer program was written which used the Lagrange five point interpolation formula (Abramowitz and Stegun, 1964) to calculate $|Z|$ as a function of frequency from 28.00 MHz to 32.00 MHz in increments of 0.01 MHz and from 56.00 MHz to 64.00 MHz in increments of 0.02 MHz.

The magnitude of Z was about 11 kΩ at the fundamental frequency and about 9 kΩ at the second harmonic frequency. The quantity in brackets in Eq. (III.4) can be neglected compared to Z at the frequencies used in these experiments. Therefore Eq. (III.4) can be approximated as

$$i_S = \frac{V_S}{|Z|} . \tag{III.6}$$

Equating i_D given by Eq. (III.3) with i_S given by Eq. (III.6) gives an equation for the displacement amplitude:

$$A = \frac{V_S S_0}{2V_b \omega C_D |Z|} . \tag{III.7}$$

The quantity A_2/A_1^2, which appears in the nonlinearity parameter β, can be written

$$\frac{A_2}{A_1^2} = \left(\frac{V_{S2}}{V_{S1}^2}\right) \frac{V_b \omega_1 C_D |Z_1|^2}{S_0 |Z_2|} \,, \tag{III.8}$$

where the subscripts 1 and 2 refer to the fundamental and second harmonic, respectively.

A block diagram of the experimental arrangement used for the measurements of the displacement amplitudes is shown in Figure III-5. A cw signal from a variable-frequency oscillator (VFO) is separated into pulses by a gated amplifier; the pulses pass through a 30 MHz bandpass filter and drive the piezoelectric quartz transducer. The pulsed signal from the capacitive receiver is sent through either a 30 MHz or 60 MHz bandpass amplifier which isolates the signal to be measured, rectifies the signal, and yields an output that is the envelope of the rectified pulse. The VFO and gated amplifier are tuned to optimize the shape and amplitude of this envelope. The output signal from the amplifier is monitored with an oscilloscope and measured with a boxcar integrator, the output of which is proportional to the time average of the input. Therefore random noise is averaged to zero while the repetitive signal adds to produce a measurable output voltage. Then the substitutional signal discussed previously is applied to the capacitive receiver and adjusted by means of attenuators and an amplifier gain control to produce the same output as that obtained from the ultrasonic pulse, as measured by the boxcar integrator. To obtain the substitutional signal at the second
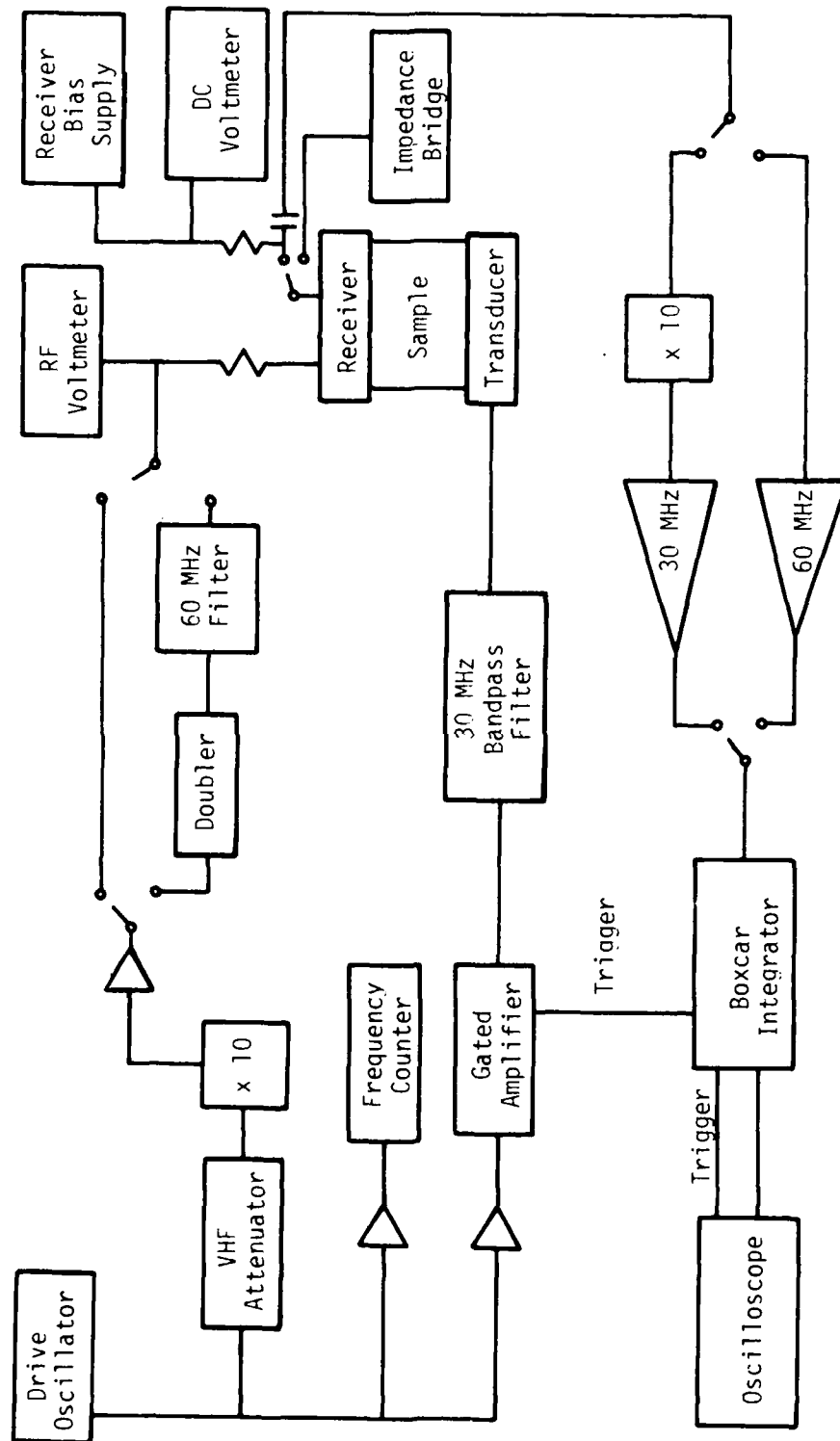
Figure III-5. Block diagram of the experimental arrangement used for the displacement amplitude measurements.

harmonic frequency, the signal at the fundamental frequency is doubled by a ring bridge mixer and filtered with a 60 MHz bandpass filter. The (RMS) voltage across the signal generator is measured with an rf volt-meter to determine v_S.

IV. THE QUARTZ TRANSDUCERS AND RECEIVING ELECTRODES

To investigate the effects of smaller diameter transducers and receiving electrodes on the amplitude measurements, several quartz transducers and receiving electrodes of various diameters were made. The diameters used in the experiments are listed on p. 35. For each of the ten electrodes of diameters 1.27-0.188 cm, a corresponding ground ring was made having inside diameter 0.1 inch (2.54 mm) greater than the diameter of the electrode. The brass receiving electrodes and ground rings were machined using standard techniques and hand lapped. The quartz transducers were reduced to the desired diameter by grinding the edge of a larger transducer (or a broken fragment if available) with a high speed ($\sim$ 20,000 rpm) silicon carbide grinding wheel. See Figure III-6. The transducer is secured to the end of a rod by attaching to the rod the adhesive from a cellulose tape in a manner similar to that described by Yost (1972, p. 36). (The polyethylene film is not necessary.) The quartz crystal is then very carefully pressed onto the end of the rod. Then the rod, whose end surface was machined to be perpendicular to the rod's axis, is placed in a collet in a milling machine. The grinding wheel is secured to the table of the milling machine. The rod and quartz crystal are slowly rotated by hand as the wheel grinds the quartz. After each revolution of the quartz crystal,

Rotate by Hand

Collet

Rod

Quartz Crystal

Grinding Wheel

Milling Machine Table

Direction of Translation
of Milling Machine Table
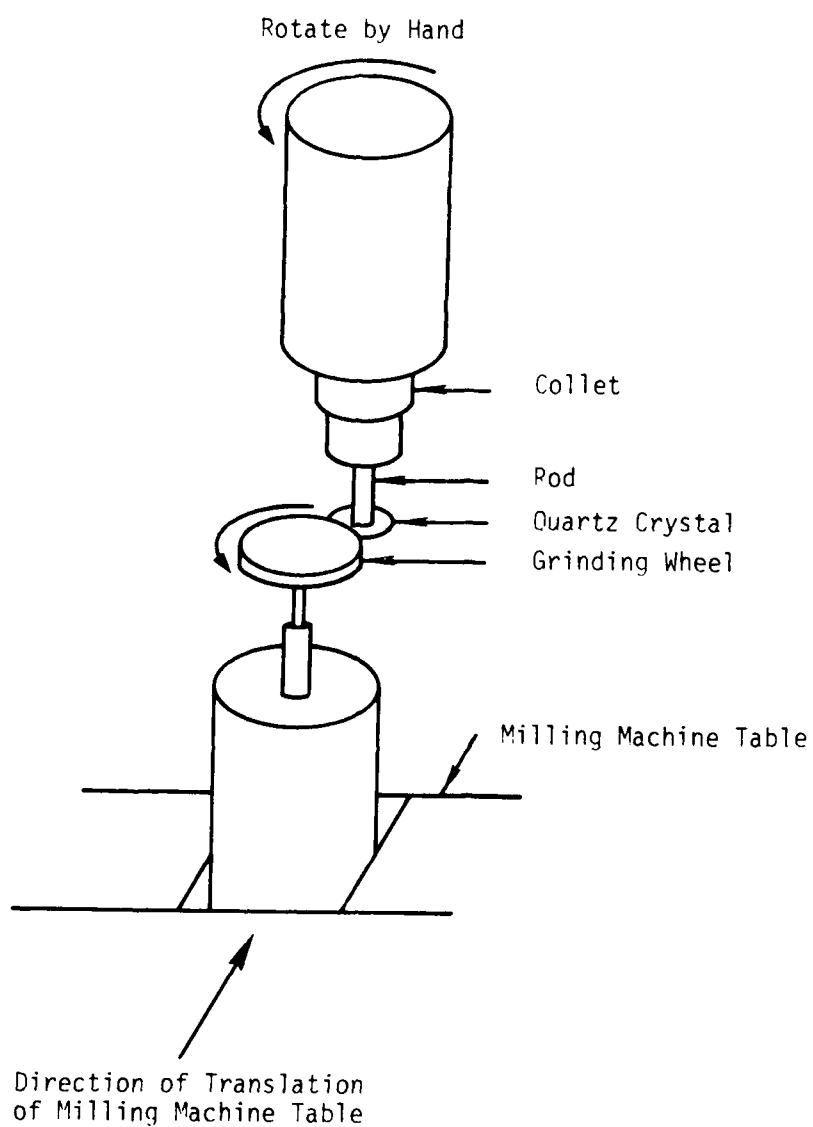
Figure III-6.   Diagram illustrating the procedure for grinding
the quartz crystal transducers.

the grinding wheel is moved slightly into the quartz using the translational motion of the table. This procedure is repeated until the desired diameter is obtained. Care should be taken in removing the quartz crystal from the rod. It may be necessary to dissolve the adhesive using a solvent such as benzene.

V. THE SAMPLES

The samples on which measurements were made included [100] and [111] copper samples, a sample of potassium zinc fluoride ($KZnF_3$) and a sample of cesium cadmium fluoride ($CsCdF_3$), each of which had faces perpendicular to the [100] and [110] directions, and a [111] $CsCdF_3$ sample. (The [111] Cu sample was used in nonlinearity measurements performed by Gauster (1966) and Peters (1968). Gauster and Peters also reported measurements on a [100] Cu sample different from the one used in the present experiments.) All of the samples are cubic crystals; copper has the face-centered cubic structure, and $CsCdF_3$ and $KZnF_3$ have the perovskite structure. The copper samples had been neutron irradiated to pin the dislocations, which reduces nonlinear effects of the dislocations. The dimensions, shapes, and crystallographic directions are shown in Figure III-7. The densities and the values of K_2 are given in Table III-1. The K_2 values for copper were calculated using the second-order elastic constants of Overton and Gaffney (1955):

$$C_{11} = 1.684 \qquad C_{12} = 1.214 \qquad C_{44} = 0.754$$
(in units of 10^{12} dynes/cm^2).

A. Cu [111]

B. Cu [100]

d = 2.54
ℓ = 3.96

d = 2.54
ℓ = 1.72

[111]

[100]

C. KZnF$_3$

[110]

[100]
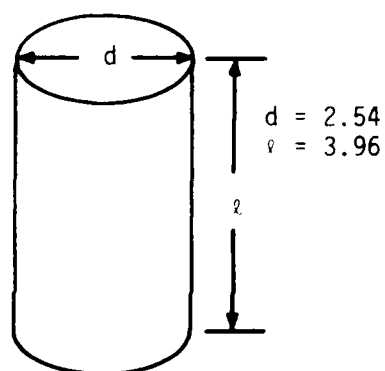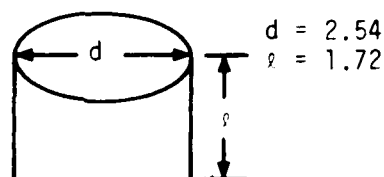
[1$\overline{1}$0]

a = 1.203
b = 1.039
c = 1.017

D. CsCdF$_3$ [100] and [110]

[100]

[110]

Imperfection
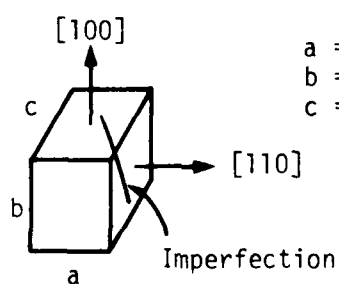
a = 1.170
b = 1.388
c = 1.197
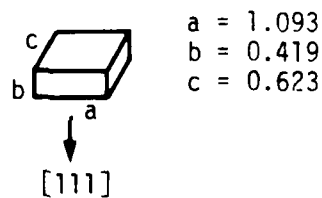
E. CsCdF$_3$ [111]

a = 1.093
b = 0.419
c = 0.623

[111]

Figure III-7. Drawings of the samples. The dimensions are given in centimeters.

Table III-1. Sample Densities and K_2 Values

Sample	Density (10^3 kg/m^3)	Direction	K_2 (10^{12} dynes/cm^2)
Cu	8.95	[100]	1.684
		[111]	2.376
CsCdF$_3$	5.638	[100]	1.08
		[110]	0.995
		[111]	0.967
KZnF$_3$	4.02	[100]	1.345
		[110]	1.317

The surfaces at the transducer and receiver ends of each sample were lapped by hand optically flat. The $CsCdF_3$ and $KZnF_3$ samples should not be touched with bare hands; they were handled using laboratory gloves. It is permissible, however, to lap these materials with an oil slurry lapping compound. This should be done carefully because the surfaces are easily scratched.

To provide a conducting surface at the transducer and receiver ends of the $CsCdF_3$ and $KZnF_3$ samples, a layer of copper of the order of 1000 $\overset{o}{A}$ thick was evaporated onto the surfaces.

The quartz transducers were bonded to all samples with Nonaq Stopcock Grease.

An imperfection of approximately ten millimeters in length exists in the ([100] and [110]) $CsCdF_3$ sample as indicated in Figure III-7.

VI. THE SEQUENCE OF THE EXPERIMENTAL INVESTIGATION

The first step taken to investigate the effects of smaller diameter transducers and receivers was to obtain data on the Cu [111] sample using four different diameter transducers with a 0.636 cm diameter receiving electrode. The diameters used for these data and the other data mentioned in this section are listed in Table III-2. Data were then obtained on the same sample using a 1.18 cm diameter receiving electrode and three different diameter transducers. Next, data were taken on the Cu [100] sample using the 0.636 cm diameter receiving electrode and four different diameter transducers. Data were then taken using transducers and receiving electrodes of equal diameter. The measurements were made on the Cu [100] sample using ten diameters.

Table III-2. Transducer and Receiver Diameters Used in the Experiments

Sample	Direction	Length (cm)	Receiver Diameter (cm)	Transducer Diameter (cm)
Cu	[111]	3.96	0.636	1.27
				0.540
				0.370
				0.195
			1.18	1.27
				0.540
				0.370
	[100]	1.72	0.636	1.27
				0.562
				0.370
				0.189
			1.27	1.27
			1.14	1.15
			1.00	1.01
			0.889	0.891
			0.764	0.766
			0.635	0.640
			0.508	0.512
			0.381	0.385
			0.254	0.258
			0.188	0.189
$CsCdF_3$	[100]		0.508	0.512
			0.381	0.385
	[110]		0.508	0.512
			0.381	0.385
	[111]		0.381	0.385
$KZnF_3$	[100]		0.508	0.512
	[110]		0.381	0.385

After determining a method for correcting the data for diffraction, measurements on $CsCdF_3$ and $KZnF_3$ were performed.

CHAPTER IV

PESULTS, DISCUSSION, AND THEORETICAL TREATMENT

OF DIFFRACTION

To perform the third-order elastic constant measurements on small
samples requires small diameter transducers and receivers. It was
anticipated that the waves emitted from the smaller transducers would
not satisfy the plane wave assumption, and the results of the measure-
ments would differ from results obtained with large diameter transducers.
In order to determine how the smaller transducers and receivers affect
the measurements, and to learn how to make a reliable determination of
third-order elastic constants from measurements made with small
diameters, data were taken as outlined in Chapter III, Section VI.

I. RESULTS OF THE MEASUREMENTS WITH UNEQUAL DIAMETER
TRANSDUCERS AND RECEIVING ELECTRODES

The results of the initial measurements on the Cu [111] sample
using two different receiving electrode sizes and a range of transducer
sizes are plotted in Figures IV-1 and IV-2. The quantities V_1 and V_2
are the voltmeter readings of the fundamental and second harmonic
voltages, respectively, and are equal to the root-mean-square values
of the input voltages. If a plane wave were incident over the full
face of the receiving electrode, according to Eq. (III.8) the quantity
$V_2/V_1{}^2$ would be proportional to $A_2/A_1{}^2$ for a given bias voltage, fre-
quency, and receiver diameter and gap spacing. Eq. (II.18) shows that

Figure IV-1. $V_2/V_1{}^2$ versus transducer diameter for the 3.96 cm Cu [111] sample using the 0.636 cm diameter receiving electrode.
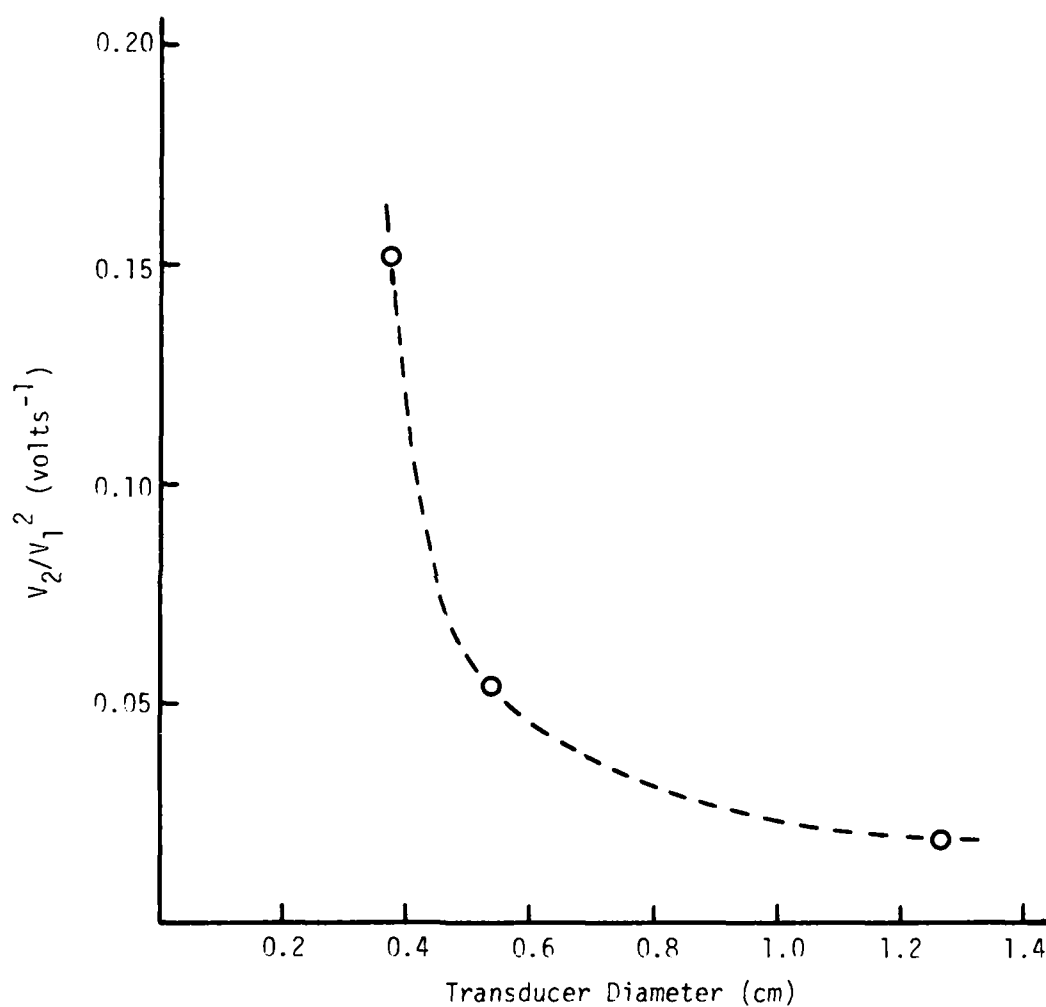
Figure IV-2. V_2/V_1^2 versus transducer diameter for the 3.96 cm Cu [111] sample using the 1.18 cm diameter receiving electrode.

the quantity $A_2/A_1{}^2$ should be constant for a given substance for a given frequency, sample length, and direction of propagation of the ultrasonic wave. Figures IV-1 and IV-2 show that the measured values of $V_2/V_1{}^2$ depend strongly on transducer diameter for a given receiver diameter. Slight differences in bias voltage, frequency, and gap spacing for the data points on a given curve would not significantly alter the curves. The results of the next set of measurements, on the Cu [100] sample of length 1.721 cm, are shown in Figure IV-3. The curve, obtained using a shorter sample and different direction of wave propagation, is flatter than the two previously discussed curves but still indicates a difference between the measurements with the smallest transducer and with the larger transducers.

Measurements performed with 12.7 mm diameter transducers have been shown to yield accepted values of the nonlinearity parameter β. The $V_2/V_1{}^2$ values in Figures IV-1 through IV-3 tend to decrease smoothly with transducer diameter and approach these accepted results. Therefore, curves such as those in Figures IV-1 through IV-3 can be used as calibration curves for obtaining the nonlinearity parameters for small samples. A family of curves for different sample lengths would be useful. To obtain the nonlinearity parameter for a given sample measured with a given diameter transducer, a correction factor would be obtained from the selected calibration curve by comparing the value on the curve at the given diameter with the value approached at the large-diameter end of the curve.
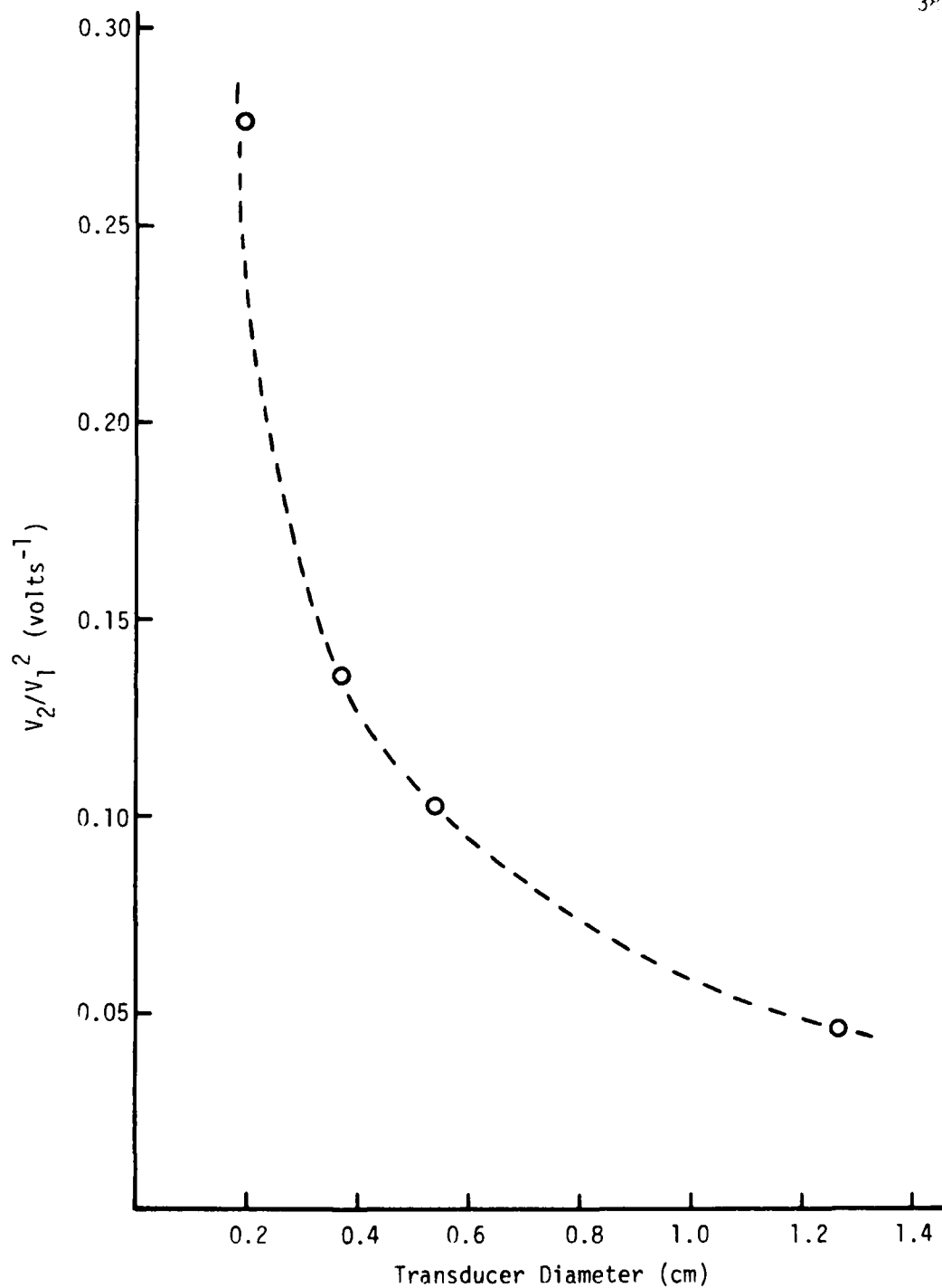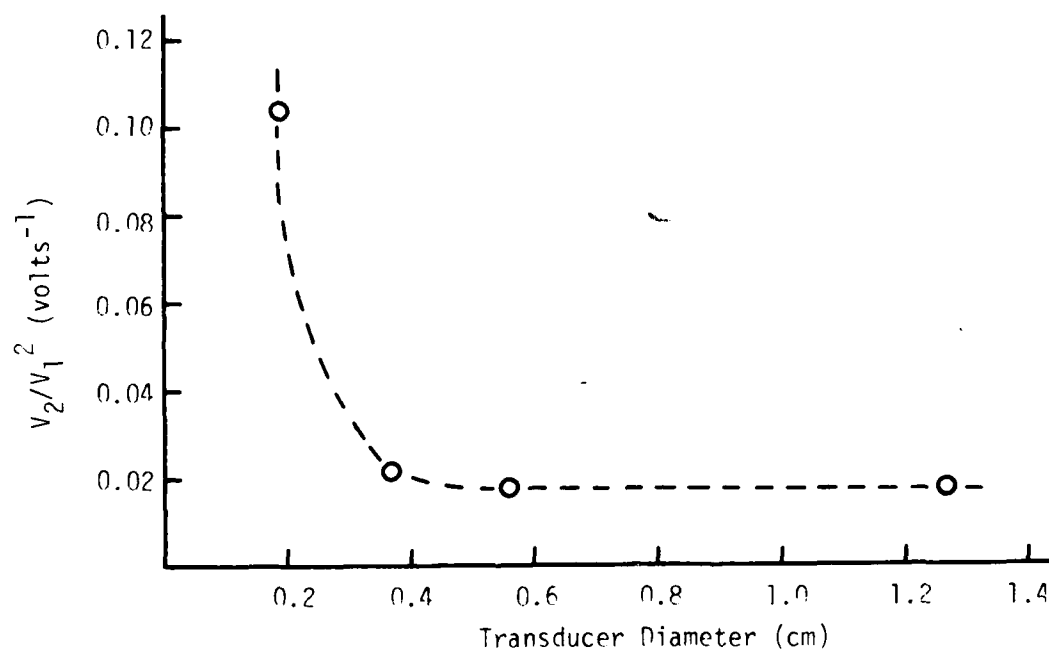
Figure IV-3. $V_2/V_1{}^2$ versus transducer diameter for the 1.72 cm Cu [100] sample using the 0.636 cm diameter receiving electrode.

II.   RESULTS OF THE MEASUREMENTS WITH EQUAL DIAMETER
TRANSDUCERS AND RECEIVING ELECTRODES

One of the objectives of the present research is to develop a
theoretical model for the nonlinear diffraction problem that is
consistent with the results. The results reported in the previous
section are not optimum for a mathematical understanding of the problem.
It was decided to obtain data using transducers and receiving electrodes
of equal diameter. This would possibly facilitate the mathematical
treatment of the problem and might allow the utilization of existing
diffraction theory for that configuration.

Ten sets of data, using the diameters listed in Table III-2,
p. 35, were taken on the 1.72 cm Cu [100] sample. For each of the ten
sets of data, a measurement was taken for ten different values of the
amplitude of the ultrasonic wave, with the exception of the measurements
made with the 1.0 cm diameter transducer and receiver, in which the
amplitude was varied through five values. Values of the fundamental
amplitude and the second harmonic amplitude were calculated for each
amplitude setting by assuming the wavefronts to have been plane, with
no correction for diffraction. These values will be denoted by A_{1u}
and A_{2u}, the subscript u meaning "uncorrected for diffraction." For
each of the ten data sets a graph of A_{2u} versus $A_{1u}^2 k^2 a$ was plotted.
The graphs for the largest and smallest diameters used, 1.27 cm and
0.189 cm, are shown in Figures IV-4 and IV-5, respectively. The
graphs for the other eight data sets are similar. The straight line
represents a linear least squares fit to the data. Each graph verifies

Figure IV-4. A_{2u} versus $A_{1u}^2 k^2 a$ for Cu [100] using the 1.27 cm diameter transducer and receiving electrode.
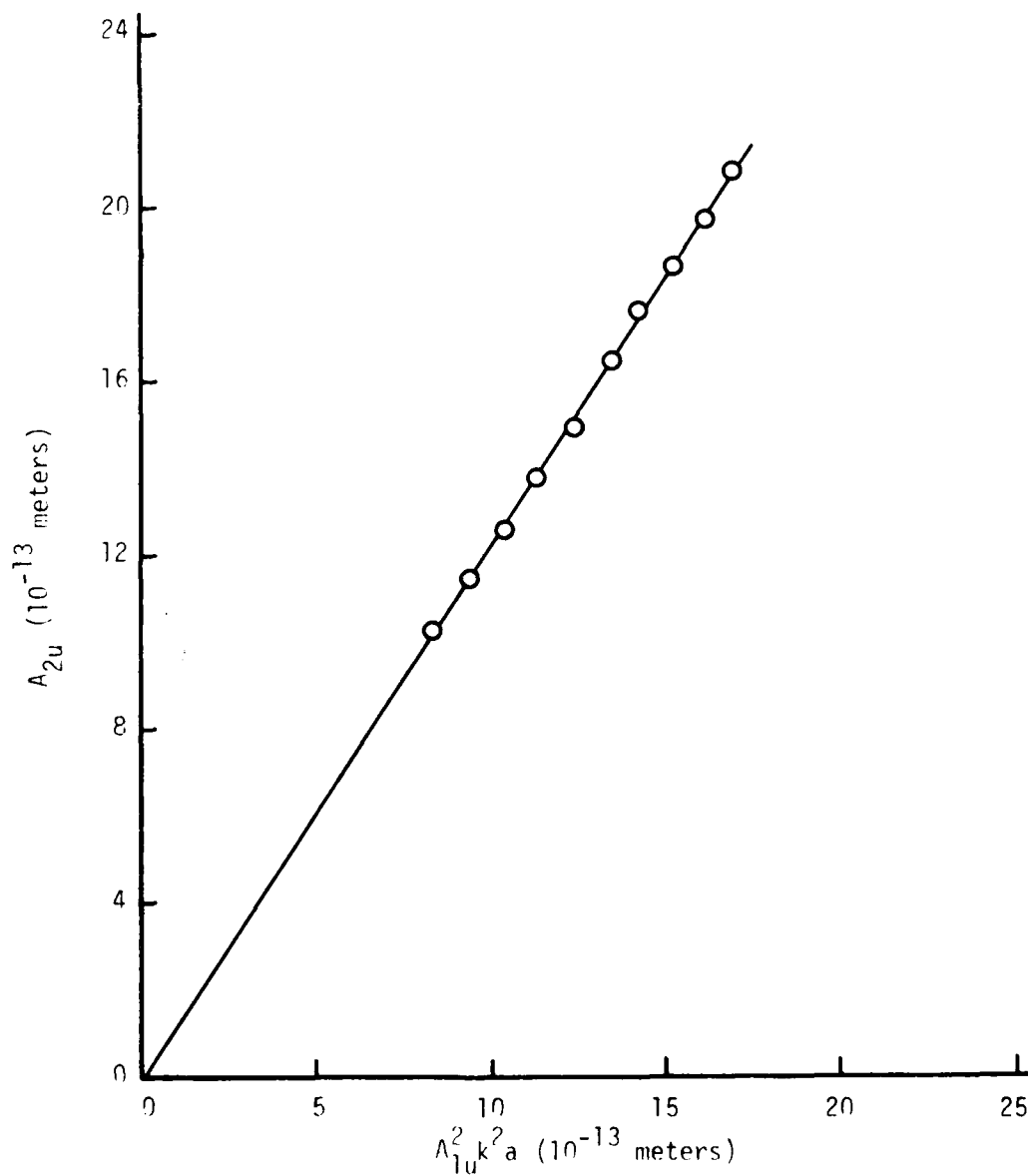
Figure IV-5. A_{2u} versus $A_{1u}^2 k^2 a$ for Cu [100] using the 0.189 cm diameter transducer and receiving electrode.

the expected proportionality of the amplitudes of the second harmonic component to the square of the amplitude of the fundamental component. The straight lines do not pass through the origin. Bains (1974) has attributed this type of result to residual noise. The present values of A_{2u} were corrected by subtracting the value of the A_{2u} intercept, calculated from a least squares linear regression formula.

The values of the nonlinearity parameter ($= 8A_{2u}/A_{1u}^2 k^2 a$) could have been calculated from the slopes of the lines in these graphs. However, Yost (1972) pointed out that a different method has the advantages of allowing measurements with good signal-to-noise ratios and yielding a value which satisfies the assumption of infinitesimal amplitude waves. In this method, the values of A_2/A_1^2 (or β) calculated for each data point are plotted as a function of A_1. A curve drawn through these data points is extrapolated to $A_1 = 0$, and the value at this point is used for the nonlinearity parameter β. This method has been particularly advantageous to previous experimenters because their data at higher values of A_1 differed significantly from the data at lower values. However, the graphs of the calculated values of β_u versus A_{1u} for the present experiments, examples of which for the 1.27 cm and 0.189 cm diameter transducers and receivers are given in Figures IV-6 and IV-7, respectively, do not show a trend in the data as a function of A_{1u}. Therefore, for each data set the nonlinearity parameter β_u was taken to be the average of the individual values.

These values for the nonlinearity parameter, which were calculated with no correction for diffraction, are plotted as a function of
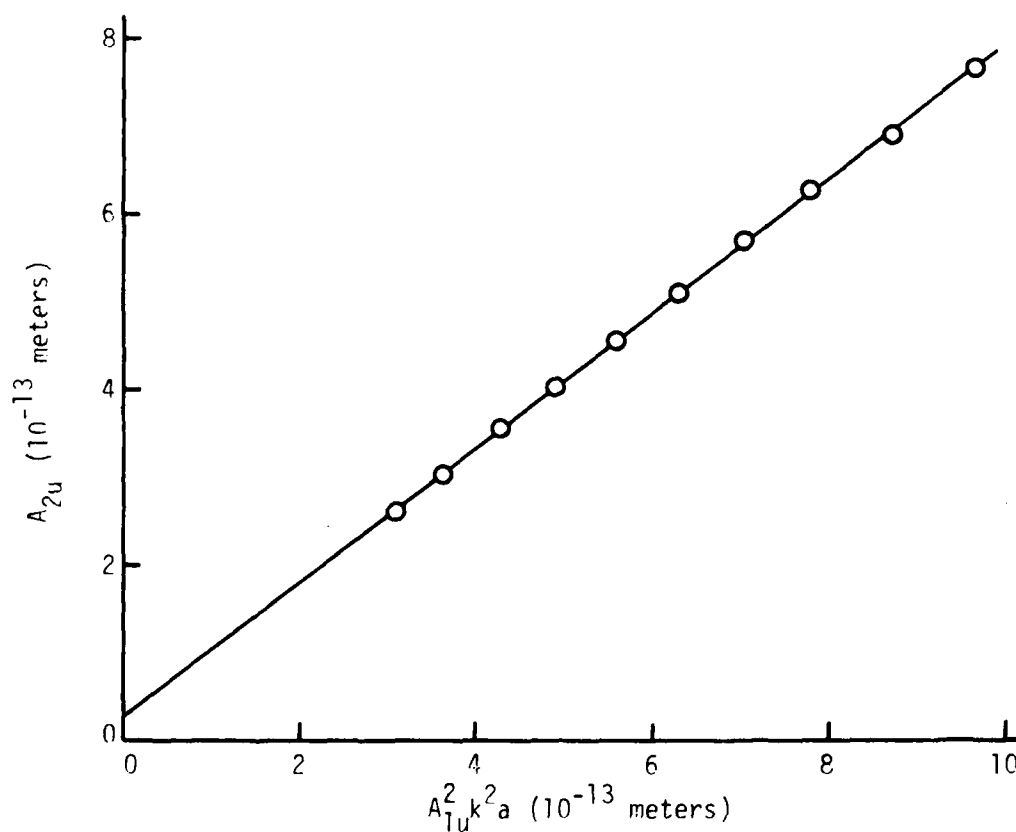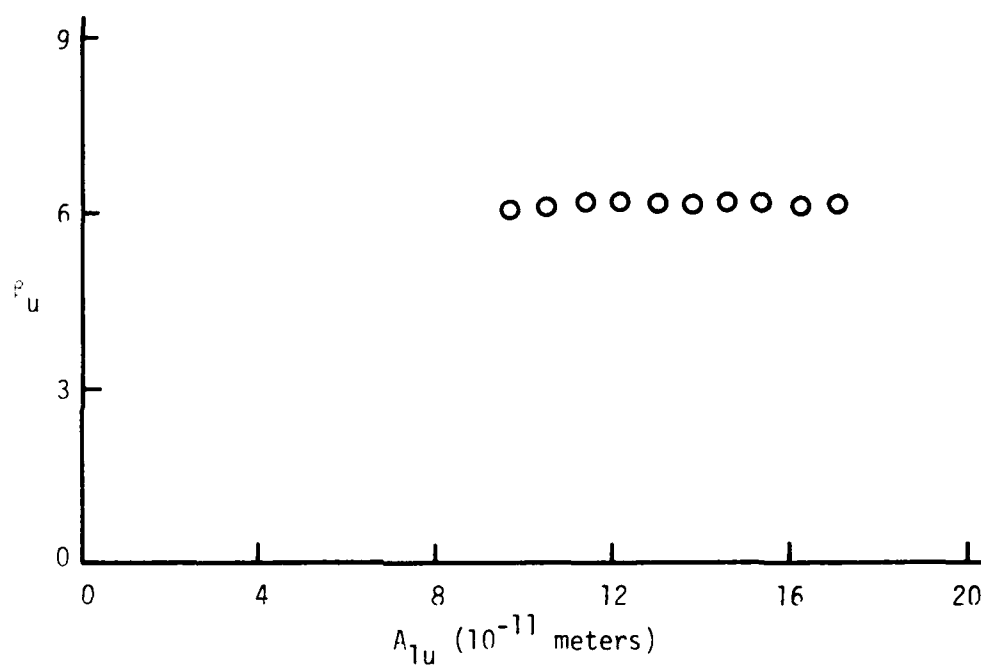
Figure IV-6. β_u versus A_{1u} for Cu [100] using the 1.27 cm diameter transducer and receiving electrode.
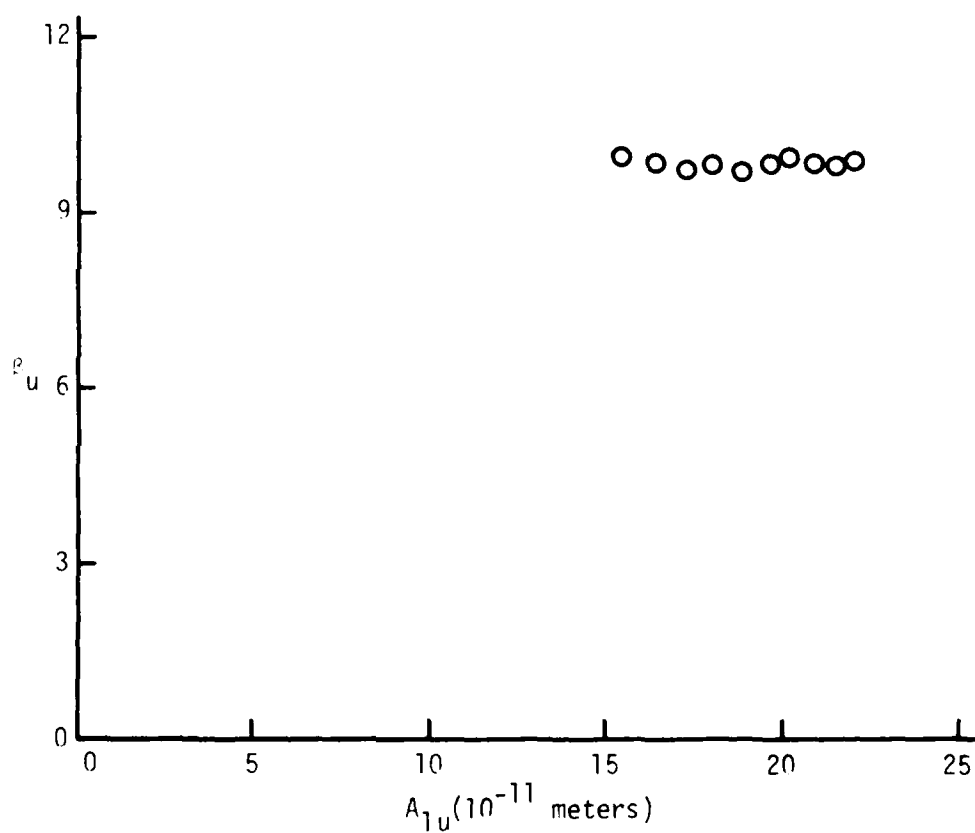
Figure IV-7. ρ_u versus A_{1u} for Cu [100] using the 0.189 cm diameter transducer and receiving electrode.

transducer and receiver diameter in Figure IV-8 and are listed on

p. 53. (There was an experimental problem in obtaining the data with

the 0.76 cm diameter transducer and receiver, and these data will not

be included in the analysis.) These values of the nonlinearity parameter

which were obtained using equal diameter transducers and receivers are

more consistent as a function of transducer diameter than were the

values obtained by varying the transducer diameter while keeping the

receiver diameter fixed. However, these β_u values still are not constant

as a function of diameter.

III. THE DIFFRACTION CORRECTION

The effects of diffraction will now be considered. In Chapter II

a theory was presented that enables one to calculate β and K_3 from

amplitude measurements of a plane wave field described by nonlinear

acoustics. It is desired to be able to determine β and K_3 for small

samples requiring small diameter transducers that emit waves that are

not plane, and to obtain a better understanding of the diffraction of

this nonlinear wave field. In the experiments, a circular transducer

oscillating at a particular frequency emits a wave into the medium.

As the wave propagates, higher harmonic components are generated. (In

the present study only the fundamental and second harmonic components

are used in the calculations.) For a plane wave, the second harmonic

component depends on the amplitude of the fundamental component, the

frequency, and the distance of propagation as stated in Chapter II.

For a wave that is not plane, it is presumed that the second harmonic
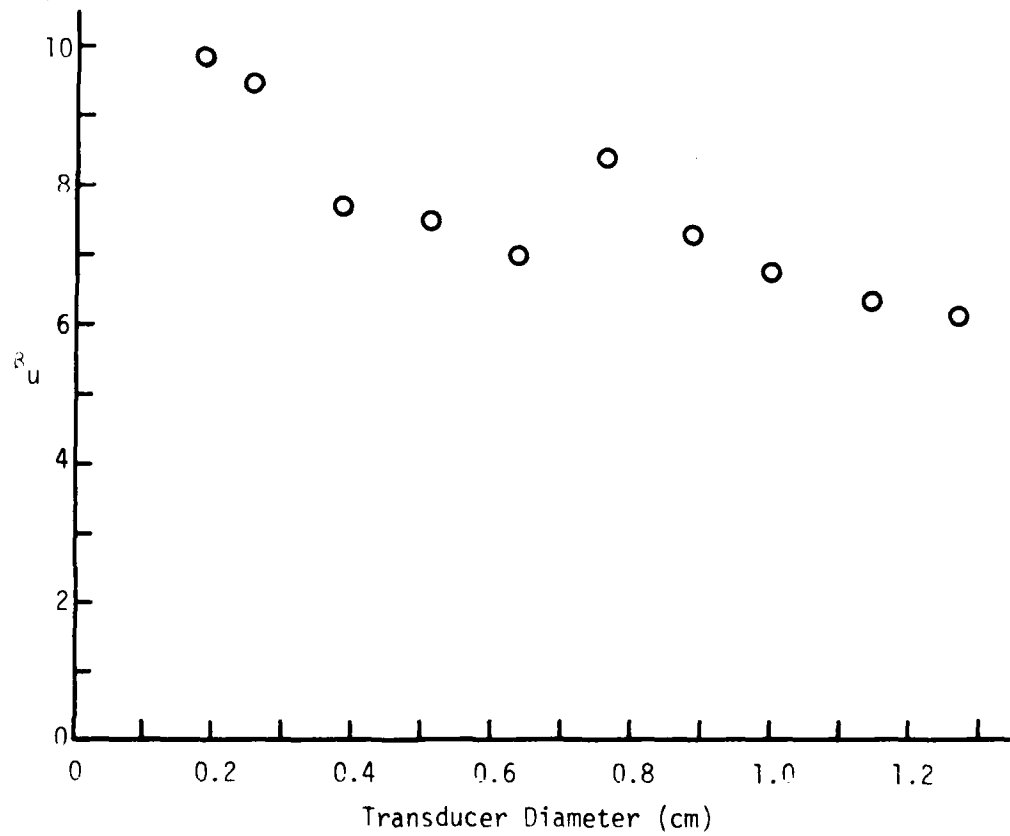
Figure IV-8. β_u versus transducer diameter for Cu [100].

also depends on these factors, but it is not known a priori what the dependence is or how to describe the diffracted nonlinear field. The diffraction correction that allows a determination of β and K_3 is the subject of this section.

The diffraction of the fundamental component will be considered first, and the second harmonic component will be treated later. By neglecting the loss of energy of the fundamental component to the second harmonic, the diffraction of the fundamental component can be treated by linear acoustics theory. The theory to be applied to the fundamental component was obtained for a homogeneous fluid medium. Analysis of data obtained with an anisotropic solid medium by utilizing a diffraction theory applicable to a fluid medium is not unprecedented; cf. Seki, Granato, and Truell (1956). [Papadakis (cf. Mason and Thurston, 1975) extended the approach used by Seki et al. to application to anisotropic solids for the linear diffraction problem.]

It is assumed that the field produced by the circular transducer in the present experiments is the same as the field produced by a plane circular piston source, set in an infinite rigid baffle and oscillating at the fundamental frequency. The diffraction correction integral is defined as the integral of the field from the piston source over the surface of a circular area of diameter equal to that of the source and coaxial with the source, divided by the integral over the same area of a plane wave field considered to be produced by an infinitely extended plane source oscillating with the same amplitude and frequency as the piston. An approximate diffraction correction integral can be obtained by integrating an approximate expression for

the piston field given by Lommel (1886). This integral, called the Lommel diffraction correction integral, denoted by D_L, has been evaluated numerically or graphically by several authors. Rogers and Van Buren (1974) evaluated the integral analytically and obtained a simple closed-form expression for it, valid at all distances from the source provided that $(kR)^{1/2} \gg 1$. Their result for the magnitude of D_L is

$$|D_L| = \{[\cos(2\pi/s) - J_0(2\pi/s)]^2 + [\sin(2\pi/s) - J_1(2\pi/s)]^2\}^{1/2}$$

(IV.1)

where

J_0 = the zero order Bessel function,

J_1 = the first order Bessel function,

$s = 2\pi z/kR^2 = z/(R^2/\lambda)$,

z = the distance from the source plane to the field plane,

k = the wavenumber,

R = radius of the piston,

λ = wavelength.

This expression for $|D_L|$ was used for correcting the data for the diffraction of the fundamental component. For each data set the value of s was calculated and $|D_L|_1$ was computed, the subscript 1 referring to the fundamental frequency component. Each nonlinearity parameter β_u was corrected by multiplying it by the square of $|D_L|_1$ since A_1^2 appears in the denominator of the expression for β. The corrected values are given by

$$\beta_{c,1} = |D_L|_1^2 \beta_u . \tag{IV.2}$$

The resulting values are denoted by $\beta_{c,1}$, the subscript c meaning "corrected" and the subscript 1 meaning that it was the fundamental component that was corrected for diffraction. The values of the quantities used in the calculations and the corrected values of the nonlinearity parameters are given in Table IV-1, in which the subscript 1 indicates that the value refers to the fundamental component. The corrected values of the nonlinearity parameters are plotted as a function of transducer diameter in Figure IV-9.

By examining Figure IV-9 it is seen that for the first time in this study the results are consistent as a function of transducer diameter. A measure of the consistency is the percent deviation of the corrected nonlinearity parameters from the mean, which is tabulated in Table IV-1. The mean value, $\overline{\beta}_{c,1}$, is 5.536.

This mean value of the corrected nonlinearity parameter values can be used to calculate K_3 by inserting $\overline{\beta}_{c,1}$ into Eq. (II.17). The result is $K_3 = (-14.4 \pm 0.3) \times 10^{12}$ dynes/cm^2. Gauster and Breazeale (1968), using a transducer having a diameter large enough that a diffraction correction was not considered necessary, obtained the value $K_3 = (-14.3 + 0.44) \times 10^{12}$ dynes/cm^2, and Peters (1968) obtained $K_3 = (-13.9 + 0.2) \times 10^{12}$ dynes/cm^2. [Gauster and Breazeale performed the calculations using the second-order elastic constants given by Hiki and Granato (1966); Peters' results and the present results were calculated using the constants given by Overton and Gaffney (1955).] There

Table IV-1. Values of the Nonlinearity Parameter Corrected for
            Diffraction of the Fundamental Component and Quantities
            Used in the Calculation*

Transducer Diameter (cm)	S_1	$|D_L|_1$	$|D_L|_1^2$	β_u	$\beta_{c,1}$	Percent Deviation From the Mean
1.27	0.0610	0.946	0.894	6.134 ± 0.039	5.484 ± 0.035	1
1.15	0.0747	0.941	0.885	6.336 ± 0.057	5.607 ± 0.050	1
1.01	0.0954	0.933	0.871	6.733 ± 0.171	5.864 ± 0.149	6
0.891	0.1236	0.924	0.854	6.269 ± 0.081	5.354 ± 0.069	3
0.640	0.2342	0.897	0.804	6.986 ± 0.075	5.617 ± 0.060	1
0.512	0.3736	0.870	0.756	7.469 ± 0.102	5.646 ± 0.077	2
0.385	0.6481	0.836	0.699	7.694 ± 0.054	5.378 ± 0.038	3
0.258	1.4434	0.748	0.559	9.461 ± 0.140	5.289 ± 0.078	4
0.189	2.6871	0.753	0.567	0.851 ± 0.081	5.585 ± 0.046	1

*Each uncertainty given is one standard deviation using (N-1) weighting.
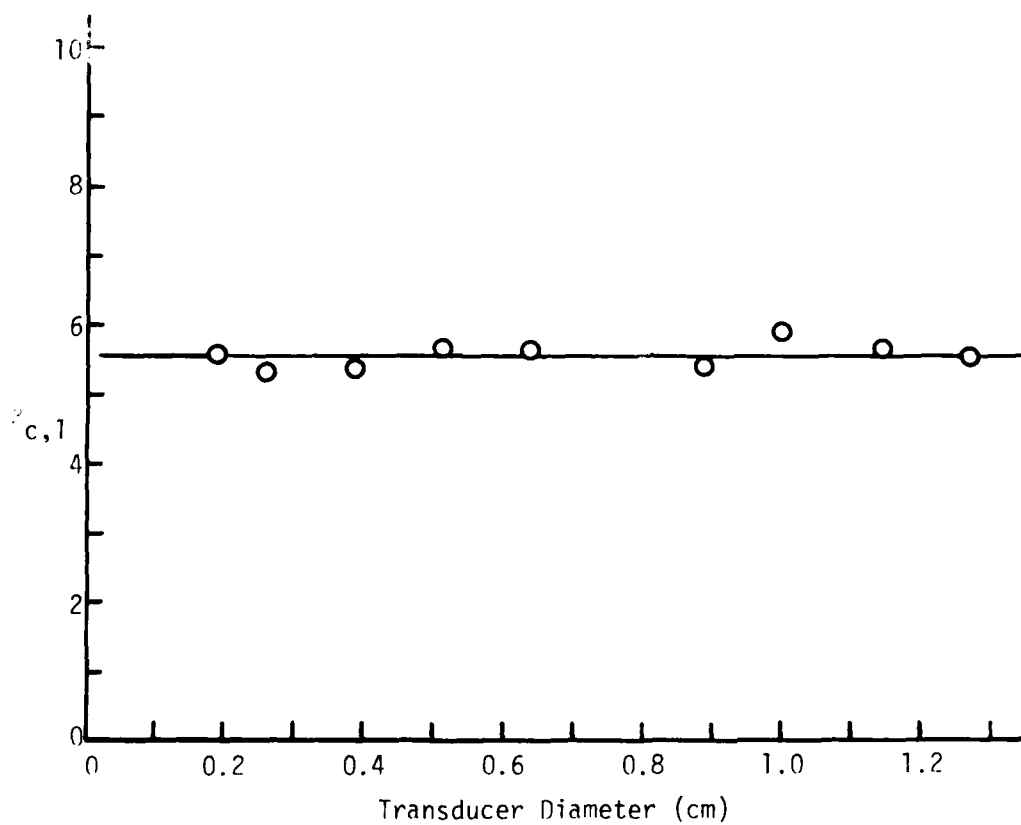
Figure IV-9. $P_{c,1}$ versus transducer diameter for Cu [100]. The straight line represents the mean value $\bar{R}_{c,1} = 5.536$.

is very good agreement between the results of the present measurements and the previous results.

By using transducers and receivers of equal diameter and correcting the data for diffraction of the fundamental field by using the Lommel diffraction correction integral, results were obtained that were consistent as a function of diameter and agreed with previous measurements.

This conclusion is encouraging; however, no correction for diffraction of the second harmonic component has been applied. A model for the diffraction of the second harmonic field allowing a diffraction correction to be calculated will now be proposed. Essentially, the Kirchhoff diffraction theory has been applied to the fundamental component. Therefore, the initial wave field can be considered to be composed of spherical Huyghens wavelets of fundamental frequency emitted from elements over the surface of the source. Each spherical wavelet generates a second harmonic component. By symmetry, the generated second harmonic wavelets must also be spherical. The amplitude of the second harmonic wavelets depends on some function of distance. An integrated value over the receiver of this second harmonic field is measured, and from this measurement the second harmonic plane wave amplitude, which will be denoted by A_{2pw}, must be determined. However, the Kirchhoff diffraction theory is valid for a field obeying the linear wave equation, so it cannot be applied directly to the generated second harmonic field.

A field that does allow determination of the second harmonic plane wave amplitude from a measurement over the receiver would be a

plane wave having amplitude A_{2pw} and frequency equal to the second

harmonic frequency, obeying the linear wave equation, passing through

an aperture of diameter equal to that of the transducer. For this

linear field the measured value over the receiver could be corrected

by the Lommel diffraction correction to calculate A_{2pw}. If it can be

shown that the measured value over the receiver of the second harmonic

field in the actual physical case is nearly the same as the measured

value over the receiver for the linear wave, then the measured value can

be corrected by the Lommel diffraction correction to obtain the second

harmonic plane wave amplitude A_{2pw}.

The value measured at the receiver depends on the phase

relationships of the second harmonic spherical wavelets and the ampli-

tudes of the wavelets. For both the physical case and the linear wave

the individual wavelets are spherical, and the frequencies of the wave-

lets are the same in the two cases. Therefore the phase relationships

are the same.

For the linear wave the amplitude of the spherical wavelets is

(A_{2pw}/r), r being the distance from the source element. In the

physical case the amplitude of the wavelets is some function of r,

divided by r. Since all the spherical wavelets reaching the receiver

travel about the same distance, the difference in amplitude between

different wavelets due to second harmonic generation is small. There-

fore the amplitude of the wavelets, at the position of the receiver,

can be approximated by a constant divided by r. This constant is equal

to A_{2pw}, and the amplitude of the wavelets is A_{2pw}/r, because that is

the amplitude the spherical wavelets of an infinitely extended plane wave would have in order to produce a plane wave of amplitude A_{2pw}. Thus the amplitudes of the wavelets for the physical case and the linear wave are nearly the same.

The values of the nonlinearity parameter obtained by correcting for diffraction both the fundamental and second harmonic components are denoted by $\beta_{c,1,2}$:

$$\beta_{c,1,2} = \frac{|D_L|_1^2 \beta_u}{|D_L|_2} = \frac{\beta_{c,1}}{|D_L|_2} . \tag{IV.3}$$

The values of $\beta_{c,1,2}$ are listed in Table IV-2 along with the values of s_2 and $|D_L|_2$, the subscript 2 referring to the second harmonic component, and the $\beta_{c,1,2}$ values are plotted as a function of transducer diameter in Figure IV-10. It is seen from the graph and the last column of Table IV-2, the percent deviation from the mean, that the values are reasonably consistent as a function of transducer diameter, except that the value obtained with the smallest (0.189 cm) diameter transducer is somewhat higher than the others. The mean of these corrected values, 6.159, is about 11% higher than the mean of the values that were corrected for diffraction of the fundamental only. Using this mean value of $\beta_{c,1,2}$ to calculate K_3, the result is $K_3 = (-15.4 + 0.8) \times 10^1$ es.cm^2.

The results obtained by correcting for diffraction of only the fundamental component were discussed earlier in this section. Those results were consistent as a function of transducer diameter and produced a value of K_3 which agreed very well with previous, accepted results.

Table IV-2. Values of the Nonlinearity Parameter Corrected for
Diffraction of Both the Fundamental and Second Harmonic
Components and Quantities Used in the Calculation*

Transducer Diameter (cm)	S_2	$\|D_L\|_2$	$\beta_{c,1,2}$	Percent Deviation From the Mean
1.27	0.0305	0.962	5.701 ± 0.036	7
1.15	0.0374	0.958	5.853 ± 0.052	5
1.01	0.0477	0.952	6.160 ± 0.156	0
0.891	0.0618	0.945	5.666 ± 0.073	8
0.640	0.1171	0.926	6.066 ± 0.065	2
0.512	0.1868	0.907	6.225 ± 0.085	1
0.385	0.3240	0.879	6.119 ± 0.043	1
0.258	0.7217	0.835	6.334 ± 0.093	3
0.189	1.3436	0.764	7.311 ± 0.060	19

*Each uncertainty given is one standard deviation using (N-1)
weighting.
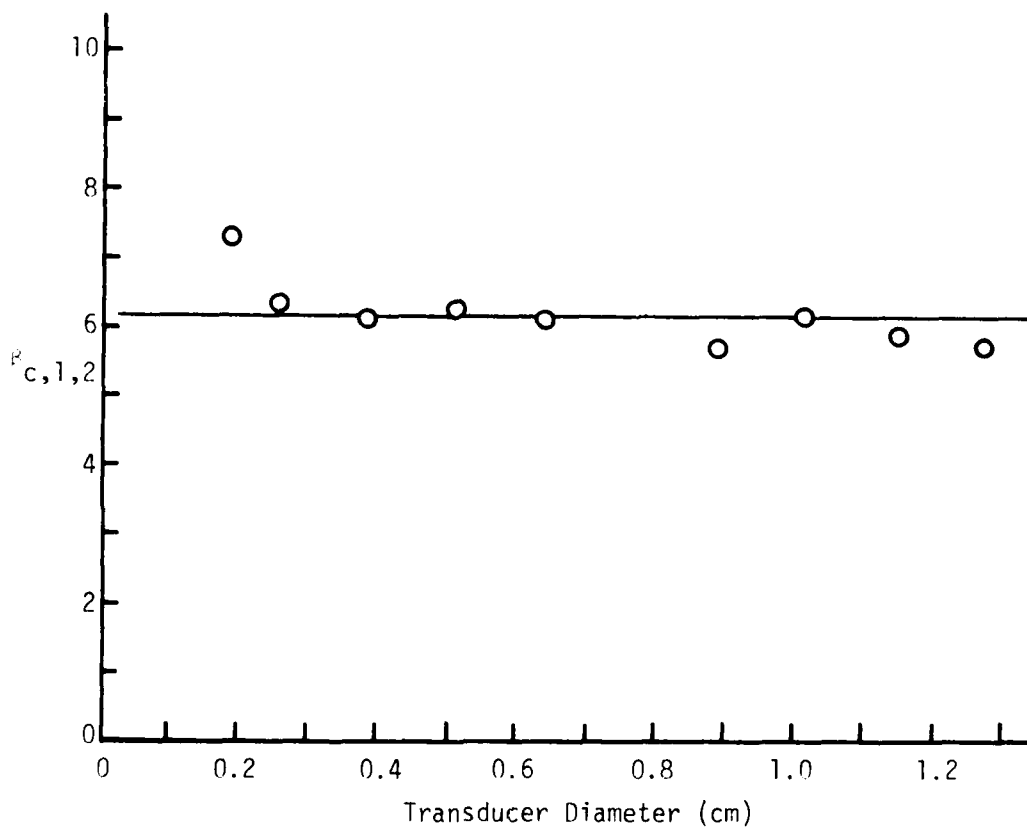
Figure IV-10. $\beta_{c,1,2}$ versus transducer diameter for Cu [100]. The straight line represents the mean value $\bar{\beta}_{c,1,2} = 6.159$.

This indicated that a correction obtained by also considering the diffraction of the second harmonic component should be small and the corrected results should be consistent as a function of transducer diameter. The proposed model for the diffraction of the second harmonic gives results which meet both of these desired conditions. The method in which only the fundamental component was corrected is considered to be the more dependable of the two correction methods.

It is seen in Figure IV-10 that, although the $\beta_{c,1,2}$ values are reasonably consistent as a function of diameter, the values appear to approach the mean value obtained with the previous correction, $\overline{\beta}_{c,1} = 5.536$, as the diameter increases. This trend tends to support the use of the correction of only the fundamental, and it indicates that the two correction methods are in good agreement for the larger diameters. The trend suggests that the theory that was used to obtain the $\beta_{c,1,2}$ values may be slightly less applicable for the smaller diameters than for the larger diameters. Also, since the values of $\beta_{c,1,2}$ for the smaller diameters are larger than the corresponding values of $\beta_{c,1}$, which agreed very well with accepted results, the second correction may be a slight overcorrection.

IV. RESULTS OF THE MEASUREMENTS ON CsCdF$_3$ AND KZnF$_3$

The samples of CsCdF$_3$ and KZnF$_3$, described in Chapter III, are small enough that the data obtained on them require corrections for diffraction. The data were taken and corrected in the same manner as the Cu [100] data. The values of A_{1u} and A_{2u}, calculated with no

correction for diffraction, are listed in Table IV-3 along with the quantity $(8A_{2u}/A_{1u}^2 k^2 a)$. Plots of A_{2u} versus $A_{1u}^2 k^2 a$ are shown in Figures IV-11 through IV-17. After correcting the A_{2u} values by subtracting the A_{2u}-intercepts, the nonlinearity parameters were calculated and plotted as a function of F_{1u} (Figures IV-18 through IV-24). As with the copper data, the uncorrected value of the nonlinearity parameter was taken to be the mean of these calculated values. The data were then corrected for diffraction of the fundamental component and for diffraction of both the fundamental and second harmonic components, as was done for the copper data. The pertinent quantities and results of the calculations for β and K_3 are listed in Table IV-4. The results of the measurements in the [100] and [110] directions in $CsCdF_3$ using two different diameter transducers are in good agreement. Notice that the percent differences between the values of K_3 obtained by correcting only the fundamental for diffraction $(K_{3(1)})$ and the values obtained by correcting both the fundamental and second harmonic $(K_{3(1,2)})$ are all less than 9%. In Table IV-5, values of combinations of third-order elastic constants are given, obtained using the correction of the fundamental component only.

The values of β and K_3 presented in Table IV-4, obtained using the diffraction correction method discussed herein, are the values that are being reported as a result of this research. It was indicated in Section IV-1 that a possible approach to determining the nonlinearity parameter of a small sample would be the use of a calibration curve. For comparison with the results given in Table IV-4, the calibration correction is discussed here. The data presented in Figure IV-8 on p. 49 is shown in Figure IV-25 with a smooth curve drawn through the

Table IV-3. Values of A_{1u}, A_{2u}, and $(8\,A_{2u}/A_{1u}^2 k^2 a)$ for $CsCdF_3$ and $KZnF_3$

Sample, Direction, Transducer Diameter (cm)	Fundamental Amplitude A_{1u} $(10^{-10}\ m)$	Second Harmonic Amplitude A_{2u} $(10^{-12}\ m)$	$\dfrac{8A_{2u}}{A_{1u}^2 k^2 a}$
$CsCdF_3$, [100], 0.512	1.493	0.891	11.998
	1.793	1.249	11.672
	2.029	1.555	11.348
	2.108	1.744	11.790
	2.364	2.215	11.907
	2.580	2.603	11.745
	2.817	3.134	11.863
	2.974	3.511	11.920
	3.152	3.935	11.899
	3.348	4.477	11.992
$CsCdF_3$, [100], 0.385	1.883	1.596	13.008
	2.043	1.853	12.838
	2.216	2.188	12.884
	2.376	2.505	12.829
	2.575	2.978	12.978
	2.709	3.324	13.095
	2.882	3.669	12.772
	3.033	4.121	12.952
	3.210	4.626	12.976
	3.370	5.104	12.992
$CsCdF_3$, [110], 0.512	1.914	0.838	7.528
	2.109	1.017	7.525
	2.310	1.201	7.407
	2.510	1.405	7.336
	2.651	1.561	7.310
	2.872	1.813	7.234
	3.012	2.041	7.402
	3.153	2.246	7.433
	3.313	2.462	7.377
	3.534	2.774	7.306
$CsCdF_3$, [110], 0.385	2.592	1.589	7.481
	2.771	1.783	7.339
	2.906	2.011	7.530
	3.081	2.234	7.442
	3.224	2.465	7.496
	3.403	2.739	7.475
	3.529	2.980	7.566
	3.681	3.222	7.516
	3.847	3.491	7.455
	3.991	3.705	7.355

Table IV-3 (continued)

Sample, Direction, Transducer Diameter (cm)	Fundamental Amplitude A_{1u} $(10^{-10}$ m)	Second Harmonic Amplitude A_{2u} $(10^{-12}$ m)	$\dfrac{8A_{2u}}{A_{1u}^2 k^2 a}$
$CsCdF_3$, [111], 0.385	1.715	0.565	16.426
	1.741	0.618	17.433
	1.802	0.650	17.124
	1.857	0.686	17.012
	1.907	0.738	17.343
	1.967	0.752	16.619
	2.013	0.802	16.937
$KZnF_3$, [100], 0.512	1.611	0.532	12.553
	1.715	0.610	12.696
	1.833	0.697	12.700
	2.003	0.838	12.786
	2.147	0.955	12.688
	2.344	1.112	12.397
	2.475	1.252	12.529
	2.618	1.393	12.449
	2.749	1.550	12.560
	2.919	1.730	12.432
$KZnF_3$, [110], 0.512	1.715	0.363	8.169
	1.839	0.421	8.231
	1.964	0.490	8.415
	2.068	0.538	8.323
	2.203	0.615	8.386
	2.328	0.684	8.363
	2.432	0.747	8.360
	2.546	0.834	8.516
	2.650	0.884	8.331
	2.775	0.964	8.294

Figure IV-11. A_{2u} versus $A_{1u}^2 k^2 a$ for CsCdF$_3$ [100] using the 0.51 cm diameter transducer and receiving electrode.
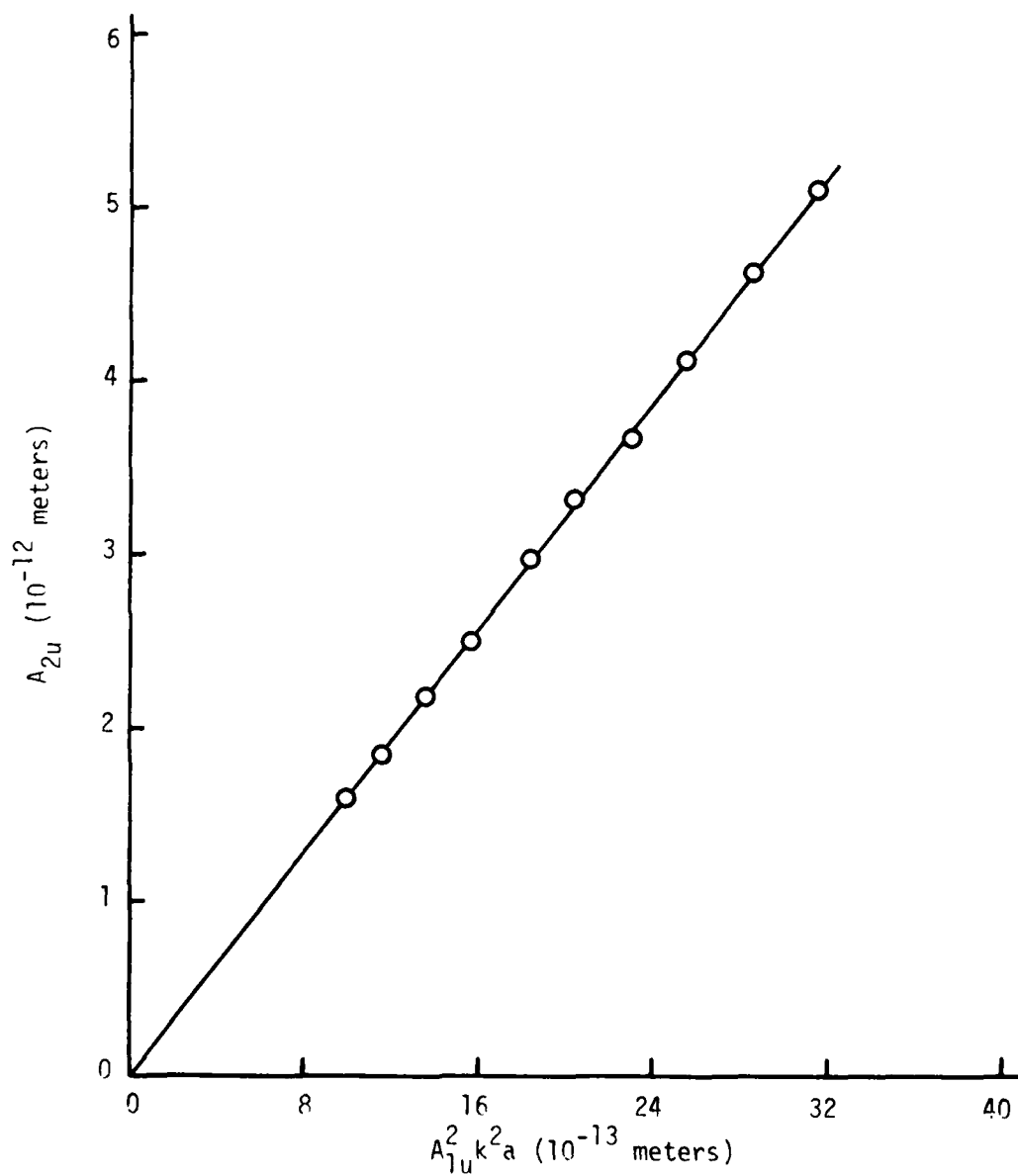
Figure IV-12. A_{2u} versus $A_{1u}^2 k^2 a$ for CsCdF$_3$ [100] using the 0.38 cm diameter transducer and receiving electrode.
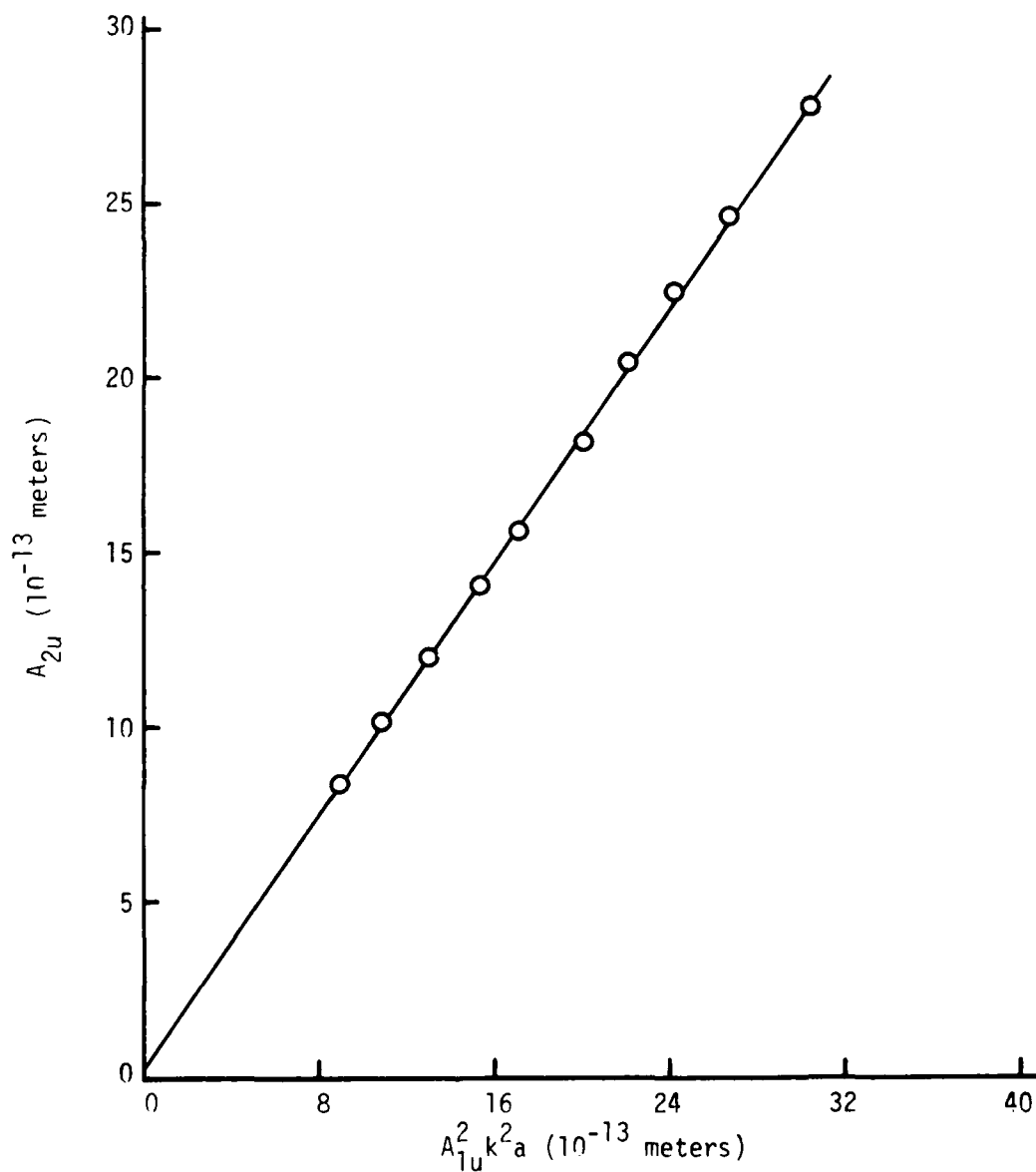
Figure IV-13. A_{2u} versus $A_{1u}^2 k^2 a$ for $CsCdF_3$ [110] using the 0.51 cm diameter transducer and receiving electrode.
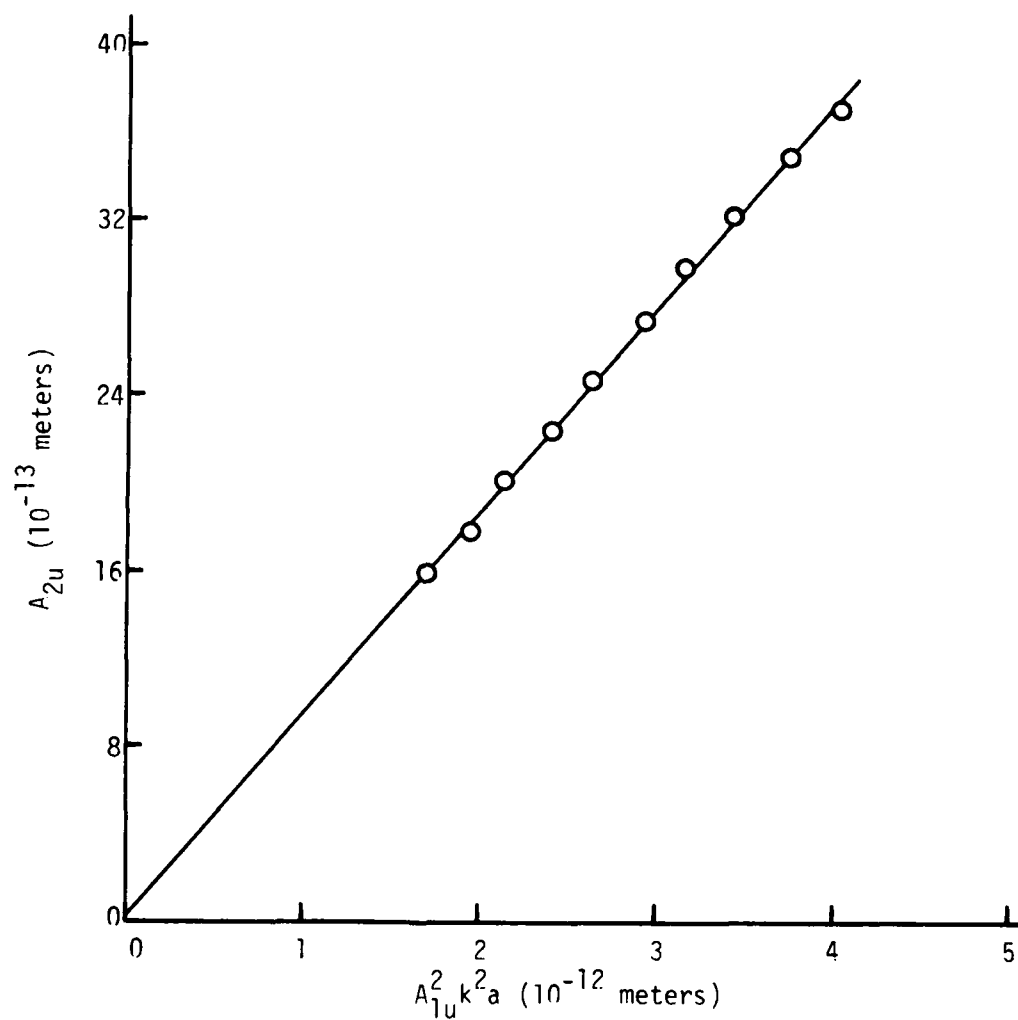
Figure IV-14. A_{2u} versus $A_{1u}^2 k^2 a$ for $CsCdF_3$ [110] using the 0.38 cm diameter transducer and receiving electrode.
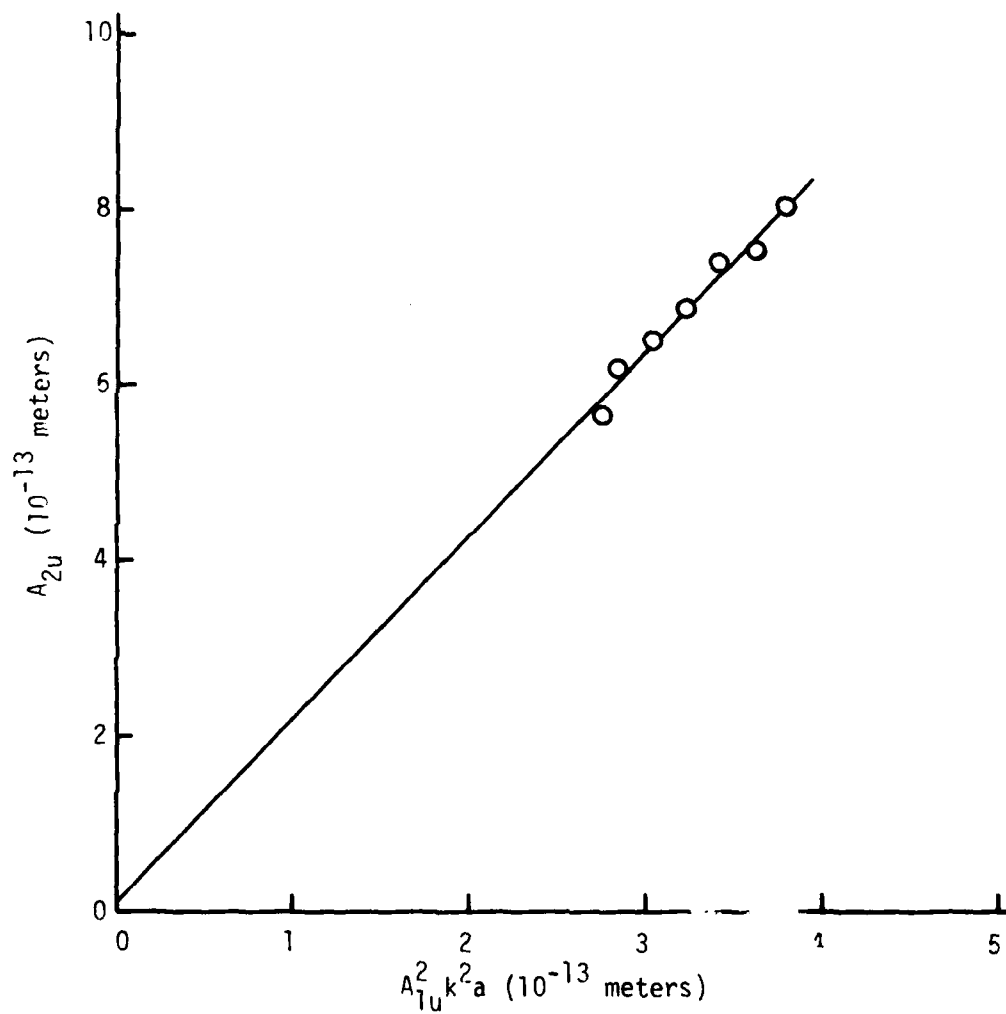
Figure IV-15. A_{2u} versus $A_{1u}^2 k^2 a$ for $CsCdF_3$ [111] using the 0.38 cm diameter transducer and receiving electrode.
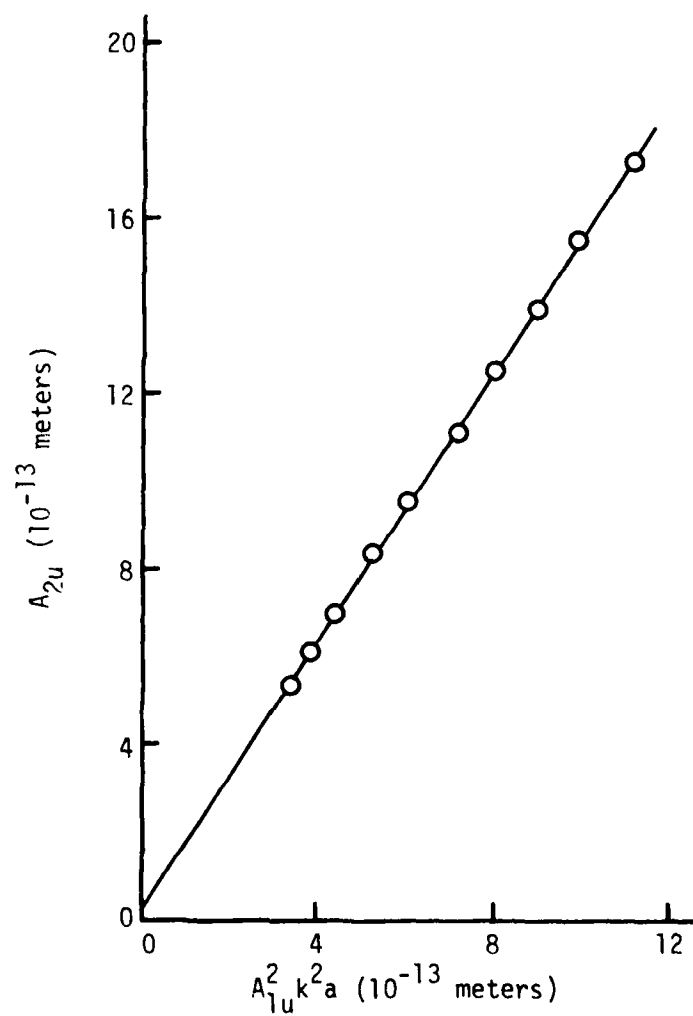
Figure IV-16. A_{2u} versus $A_{1u}^2 k^2 a$ for KZnF$_3$ [100] using the 0.51 cm diameter transducer and receiving electrode.
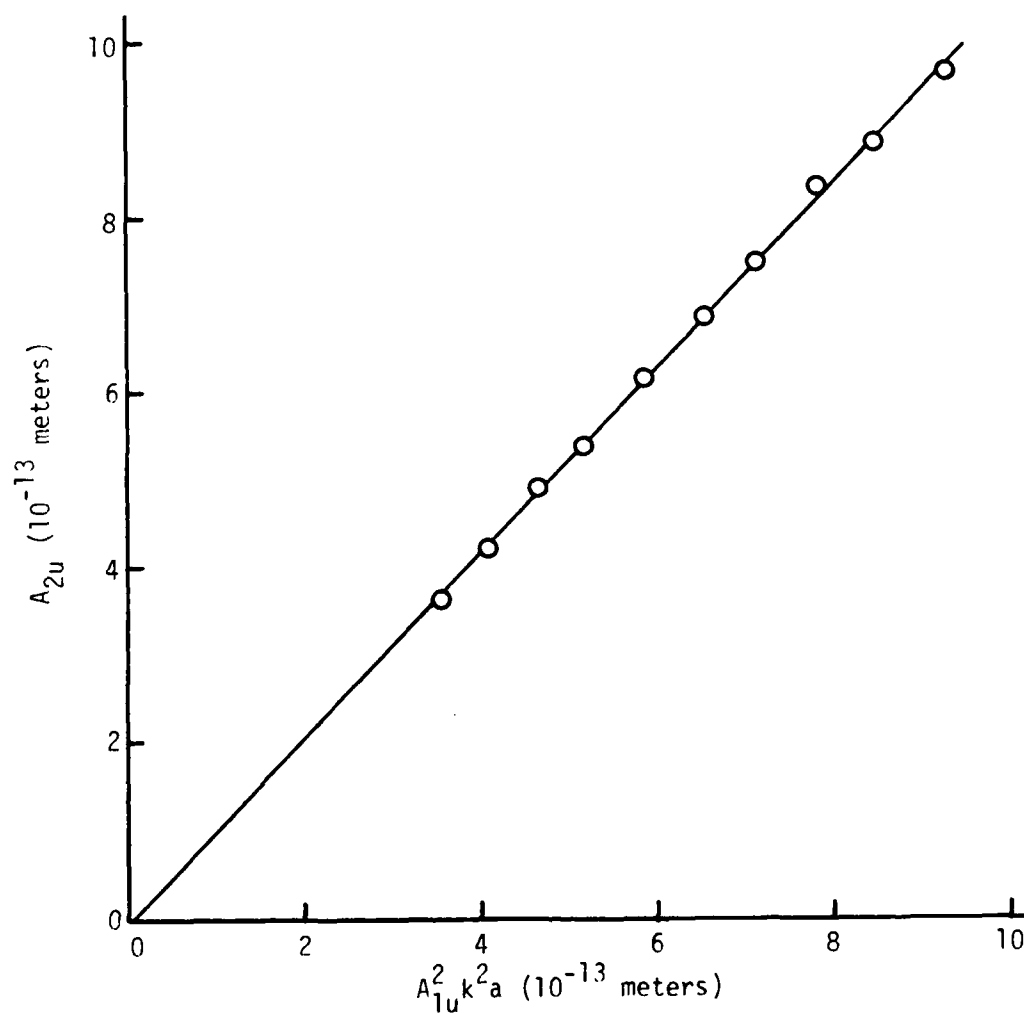
Figure IV-17. A_{2u} versus $A_{1u}^2 k^2 a$ for $KZnF_3$ [110] using the 0.38 cm diameter transducer and receiving electrode.
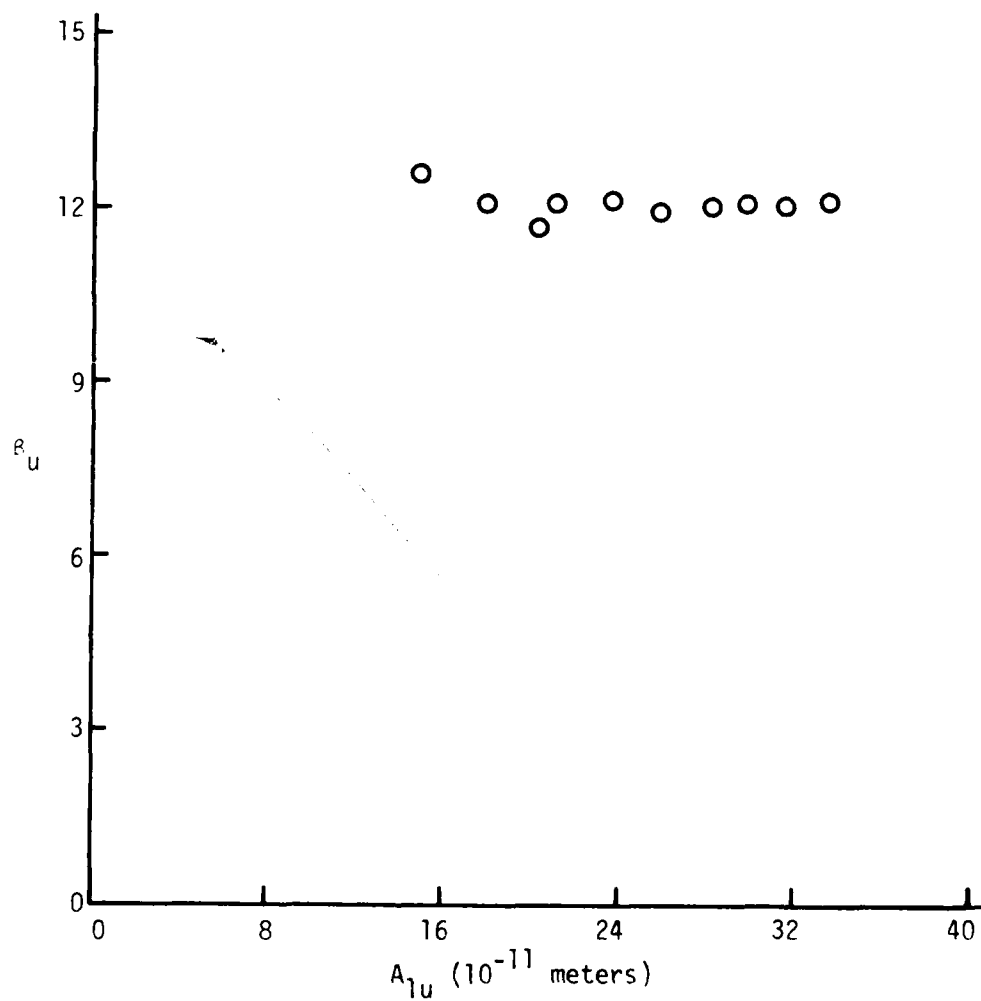
Figure IV-18. β_u versus A_{1u} for $CsCdF_3$ [100] using the 0.51 cm diameter transducer and receiving electrode.
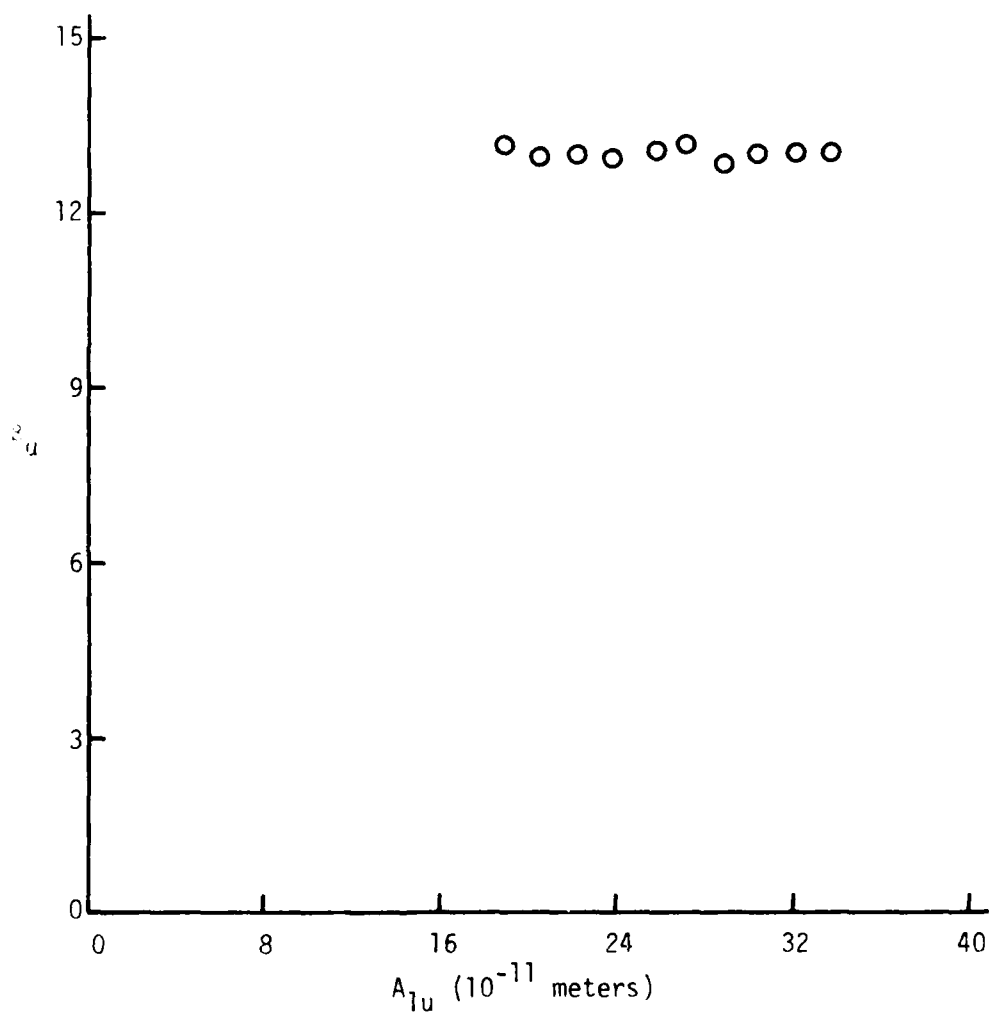
Figure IV-19. ρ_u versus A_{1u} for $CsCdF_3$ [100] using the 0.38 cm diameter transducer and receiving electrode.
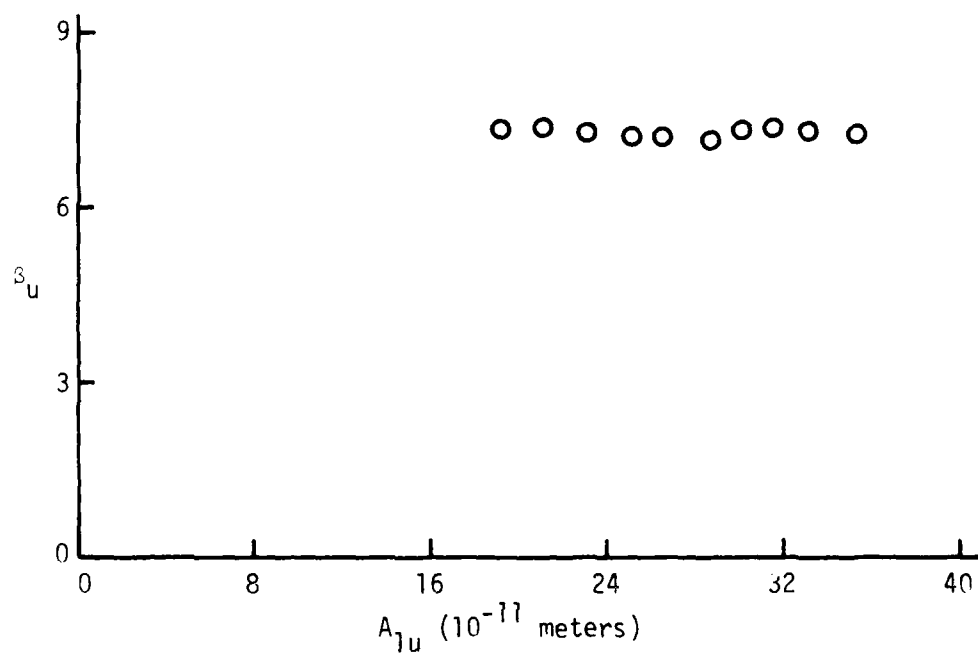
Figure IV-20. β_u versus A_{1u} for $CsCdF_3$ [110] using the 0.51 cm diameter transducer and receiving electrode.
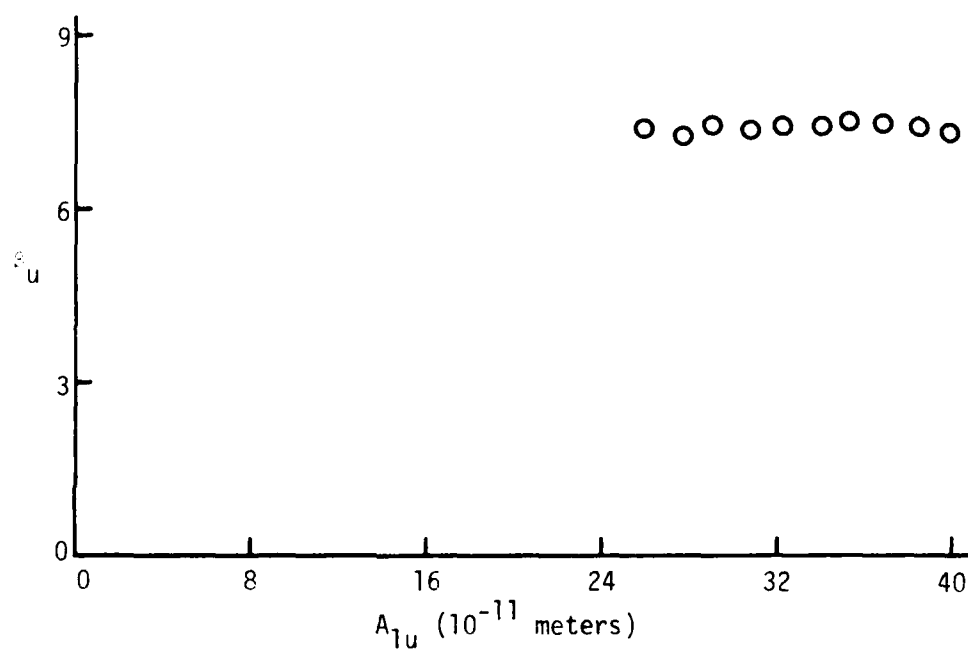
Figure IV-21. β_u versus A_{1u} for $CsCdF_3$ [110] using the 0.38 cm diameter transducer and receiving electrode.
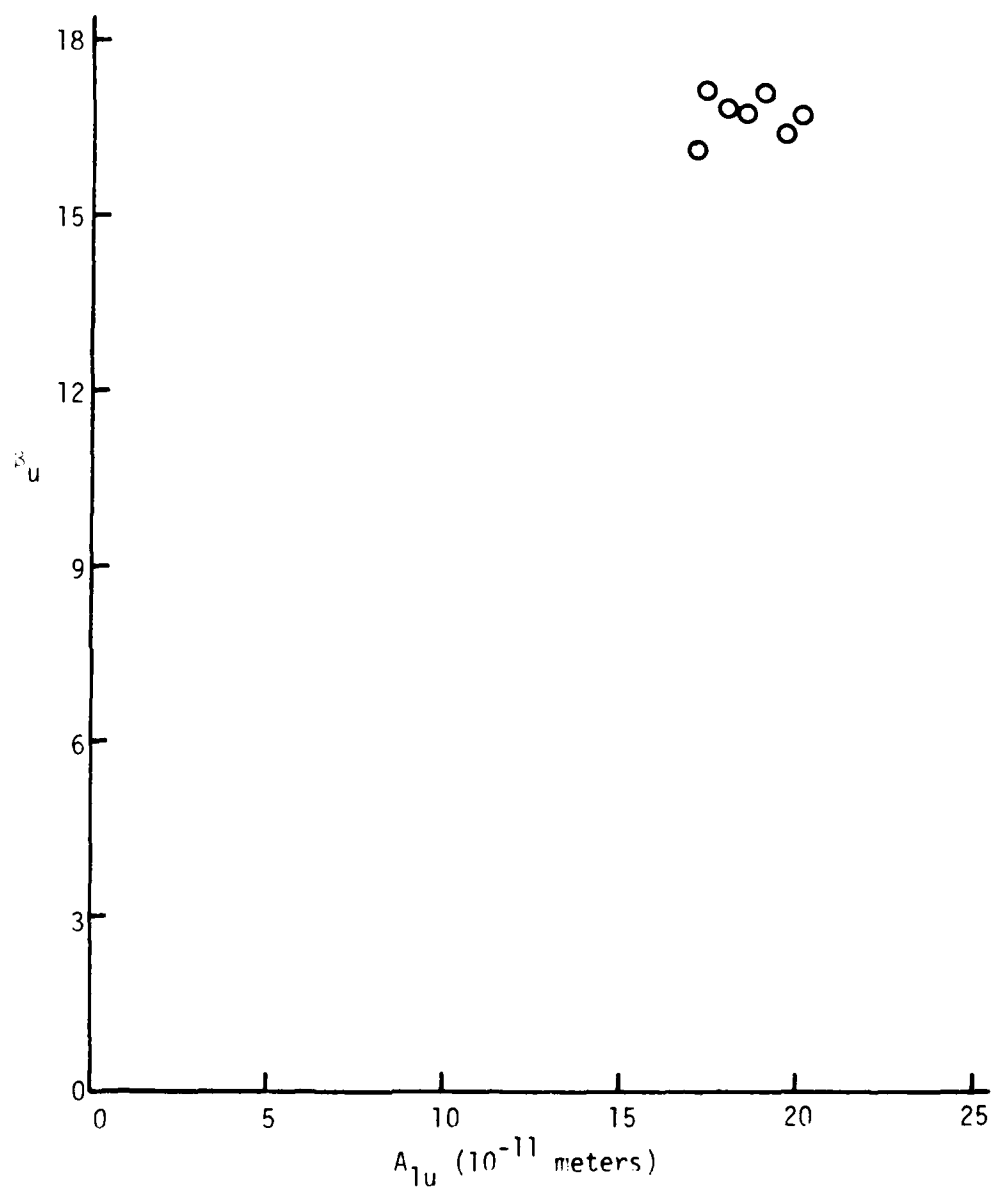
Figure IV-22. P_u versus A_{1u} for $CsCdF_3$ [111] using the 0.38 cm
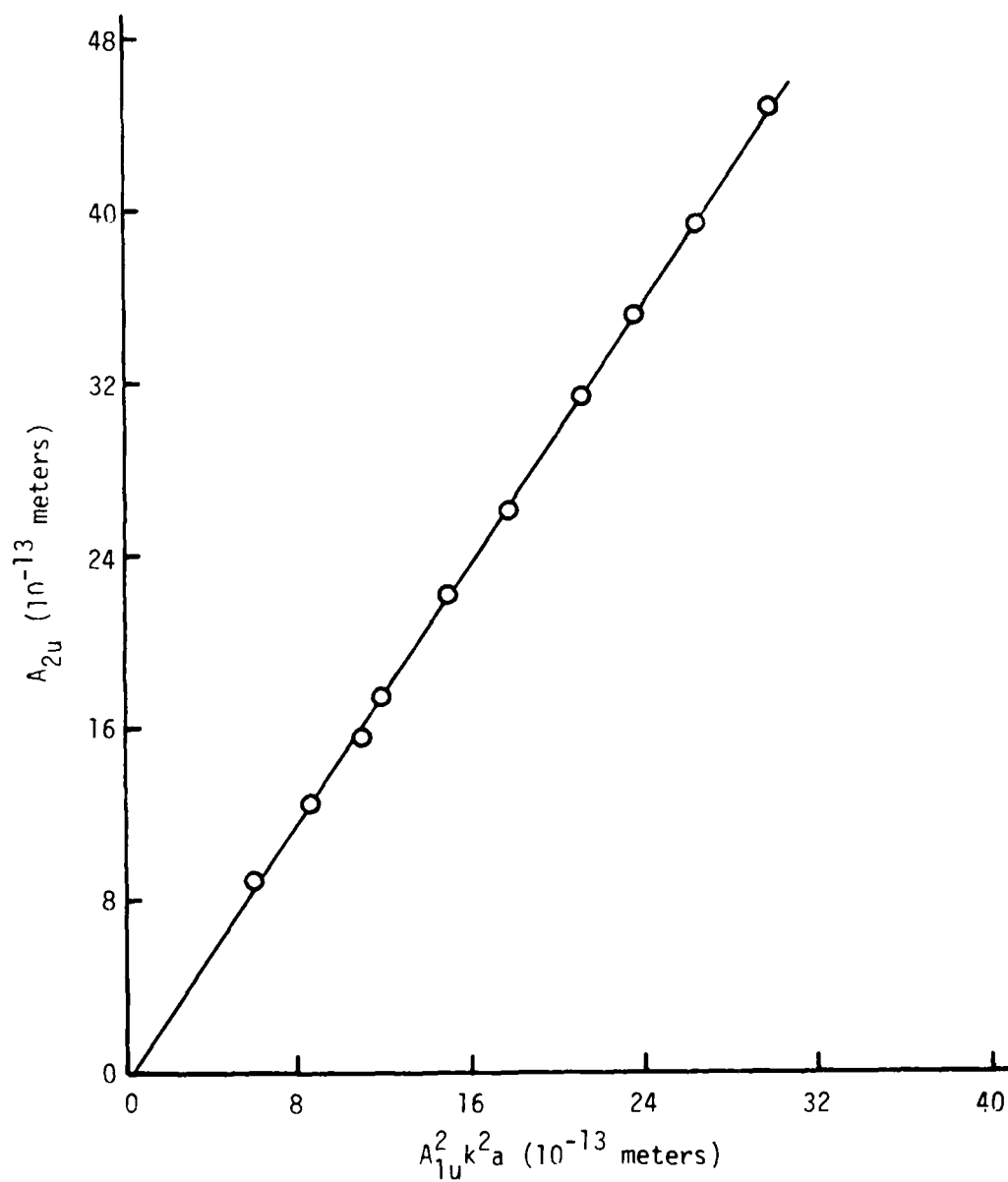diameter transducer and receiving electrode.
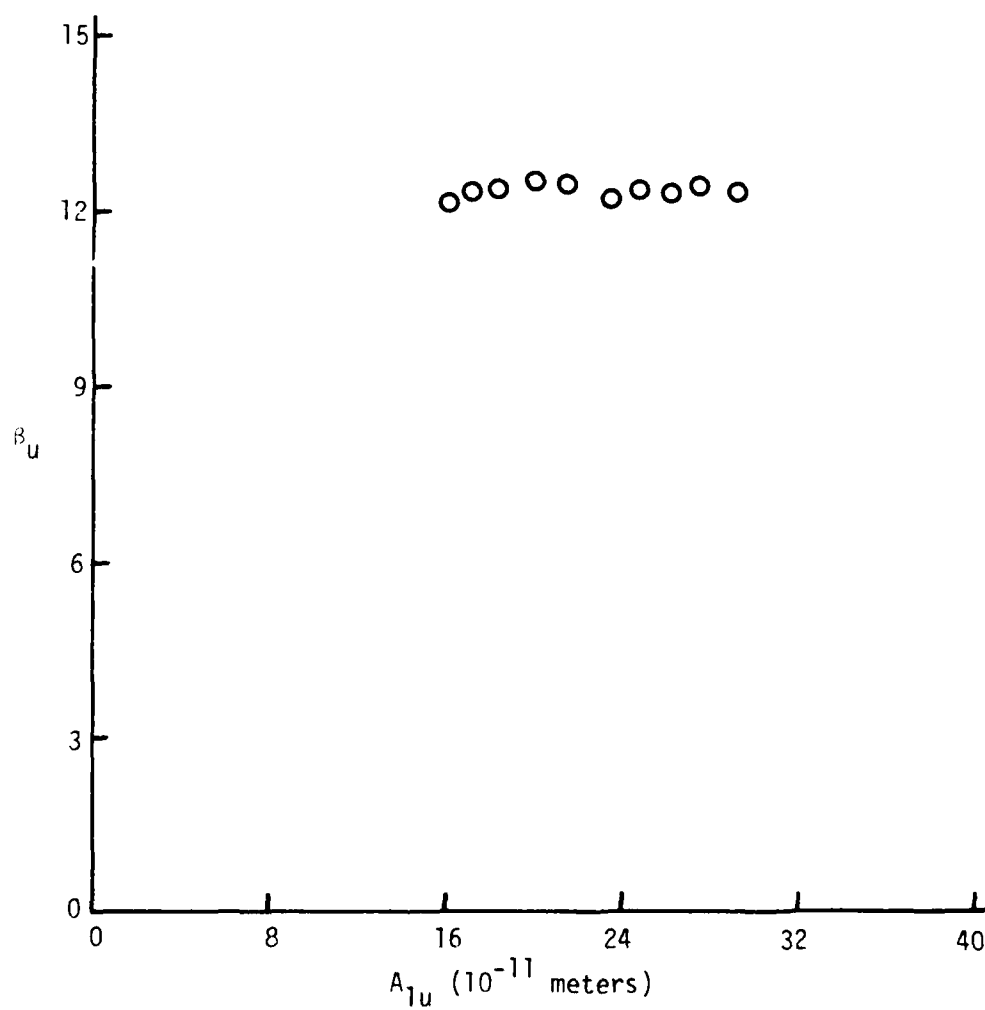
Figure IV-23. β_u versus A_{1u} for $KZnF_3$ [100] using the 0.51 cm diameter transducer and receiving electrode.
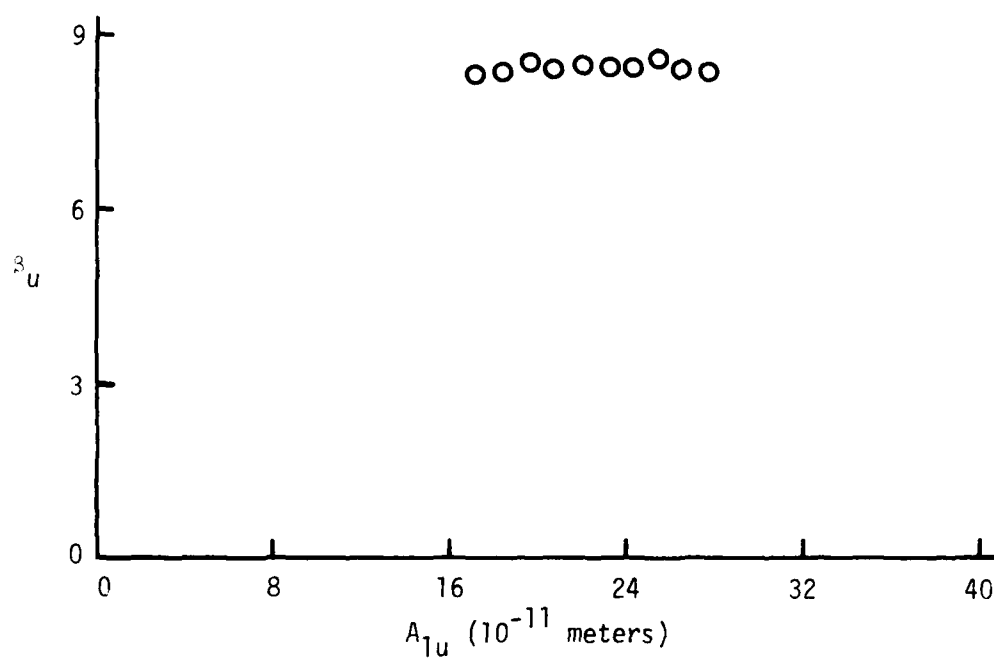
Figure IV-24. β_u versus A_{1u} for $KZnF_3$ [110] using the 0.38 cm diameter transducer and receiving electrode.

Table IV-4. Results of the Measurements on CsCdF$_3$ and KZnF$_3$ and Quantities Used in the Calculations*

Direction	CsCdF$_3$					KZnF$_3$	
	[100]	[100]	[110]	[110]	[111]	[100]	[110]
Transducer Diameter (cm)	0.512	0.385	0.512	0.385	0.385	0.512	0.512
S_1	0.3038	0.5271	0.2460	0.4266	0.1504	0.3501	0.2921
$\rho_{L,1}$	0.883	0.855	0.895	0.866	0.916	0.878	0.887
$\rho_{L,1,2}$	0.781	0.730	0.800	0.750	0.839	0.771	0.787
S_2	0.1519	0.2635	0.1230	0.2133	0.0752	0.1750	0.1461
$\rho_{L,2}$	0.916	0.891	0.924	0.901	0.940	0.910	0.917
C_u	12.1 ± 0.22	13.0 ± 0.10	7.28 ± 0.07	7.41 ± 0.07	17.0 ± 0.37	12.3 ± 0.11	8.42 ± 0.08
$C_{c,1}$	9.43 ± 0.18	9.50 ± 0.07	5.83 ± 0.06	5.56 ± 0.06	14.3 ± 0.31	9.51 ± 0.09	6.63 ± 0.07
$C_{c,1,2}$	10.3 ± 0.19	10.7 ± 0.08	6.31 ± 0.06	6.17 ± 0.06	15.2 ± 0.33	10.4 ± 0.10	7.23 ± 0.07
$K_3(1)$ ($\times 10^{12}$ dyn/cm^2)	-13.4 ± 0.19	-13.5 ± 0.08	-8.78 ± 0.06	-8.52 ± 0.06	-16.7 ± 0.30	-16.8 ± 0.12	-12.7 ± 0.09
$K_3(1,2)$ ($\times 10^{12}$ dyn/cm^2)	-14.4 ± 0.21	-14.8 ± 0.09	-9.26 ± 0.06	-9.13 ± 0.06	-17.6 ± 0.32	-18.1 ± 0.13	-13.5 ± 0.09
Percent Difference in $K_3(1)$ and $K_3(1,2)$	7	9	5	7	5	7	6

*Each uncertainty given is one standard deviation using (N-1) weighting.

Table IV-5. Measured Values of Combinations of Third-Order Elastic Constants of $CsCdF_3$ and $KZnF_3$ in Units of 10^{12} dyn/cm^2

Sample	C_{111}	$(C_{112} + 4C_{166})$	$(6C_{144} + C_{123} + 8C_{456})$
$CsCdF_3$	-13.4	- 7.24	-46.6
$KZnF_3$	-16.8	-11.3	
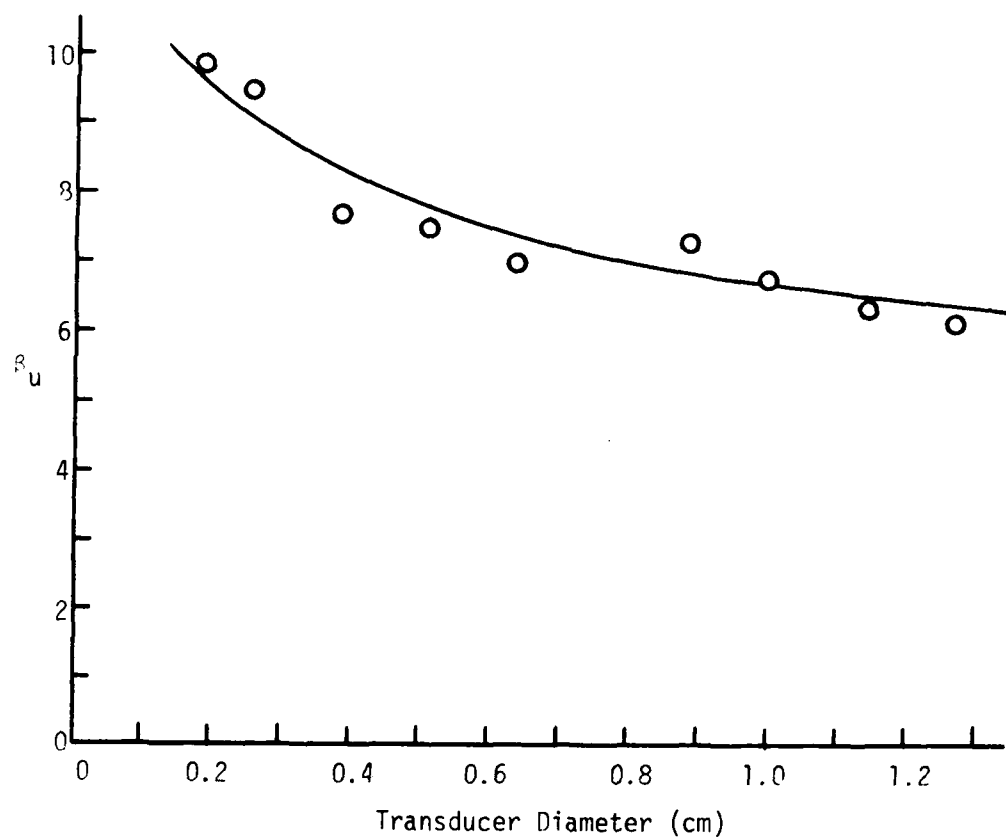
Figure IV-25. β_u versus transducer diameter for Cu [100]. The smooth curve can be used as a calibration curve.

data points. The data approach a value of the nonlinearity parameter

of approximately 5.5. The smooth curve can be used to approximate

a correction factor for data obtained using a transducer-receiver

pair of given diameter. The values on the smooth curve at 0.385 cm

and 0.512 cm, the diameters used for the measurements on $CsCdF_3$ and

$KZnF_3$, are ~8.3 and ~7.8. The correction factor would be 5.5/8.3 = .66

for the 0.385 cm diameter and 5.5/7.8 = .71 for the 0.512 cm diameter.

The correction factors obtained from the Lommel diffraction correction,

$|D_L|_1^2$ in Table IV-4, range from 0.730 to 0.839 for the 0.385 cm

diameter and from 0.771 to 0.800 for the 0.512 cm diameter. The values

of K_3 calculated from the calibration correction factors, listed in the

same order as that in Table IV-4, are -12.5, -12.5, -8.13, -7.85, -13.7,

-15.8, and -11.8, in units of 10^{12} dynes/cm^2. The correction factors

obtained from the calibration curve do not take into account the length

of the sample or the wavelength of a given frequency wave in the

material. These quantities are taken into account by the Lommel

diffraction correction.

V. ESTIMATE OF THE DIMENSIONS OF THE SMALLEST MEASURABLE SAMPLE

It is useful to estimate the dimensions of the smallest sample

measurable by the present technique. The minimum dimension transverse

to the direction of wave propagation is approximately 5 mm; this allows

the sample walls to be sufficiently outside the ultrasonic beam and is

large enough for measurement with the 0.19 cm transducer and receiver.

Equation (II.15) shows that the amplitude of the second harmonic

component in a plane wave is directly proportional to the length of the
sample and depends on the quantities K_2 and K_3; thus the sample must be
long enough to allow a measurable second harmonic to be generated, and
this minimum length will depend on the material being measured. It is
estimated that this minimum length would be typically of the order of
4 mm.

It may not be possible to perform the measurements on a sample
having both the minimum transverse dimension and minimum length given
above. Measurement of smaller amplitudes tends to require larger
diameter transducer-receiver sets. For example, the [111] $CsCdF_3$ sample
of length 4.19 mm was measured with the 0.38 cm diameter transducer and
receiver, but data could not be obtained using the 0.19 cm or the
0.26 cm diameter transducer and receiver.

VI. ERROR ANALYSIS

The primary sources of systematic error are the measurement of
the substitutional signal voltage and the measurement of the impedance
of the resistor in the base of the capacitive detector housing as a
function of frequency. It is estimated that the systematic error for
the measurement of β_u is within $\pm 12\%$. After correction of β_u for
diffraction, the mean value $\bar{\beta}_{c,1}$ agreed very well with previous, accepted
results (see Section IV-III), and the largest deviation of any of the
nine $\beta_{c,1}$ values from $\bar{\beta}_{c,1}$ was 6% (see Table IV-1, p. 53). Therefore
the error introduced into the determination of the nonlinearity
parameter by the diffraction correction appears to be relatively small,

since the error of the $\beta_{c,1}$ values was well within the ±12% systematic error in each case.

VII. SOME PROBLEMS ASSOCIATED WITH THE APPLICATION OF DIFFRACTION THEORY TO THE PRESENT MEASUREMENTS

The nonlinear wave equation (II.13) that has been used to describe the wave propagation is valid only for a pure longitudinal mode plane wave. It was obtained from the general equation, (II.12), by assuming that the only component of displacement, say u_1, is along the pure mode direction, so that $u_2 = u_3 = 0$, and that u_1 is a function only of a_1 and t. However, in the diffraction problem the displacement also includes the components u_2 and u_3, and each displacement component is a function of a_1, a_2, a_3, and t. Thus Eq. (II.12) contains many terms in the general case which are not present when considering only pure longitudinal plane waves. From Eq. (II.12) three long coupled equations are obtained, one for each of the directions labelled 1, 2, 3 [see Gauster (1966)]. An attempt to solve the general equations would be complicated, and would involve nonpure mode propagation.

The previously discussed theory that was used for the diffraction correction was developed assuming the medium to be a homogeneous fluid. The measurements of third-order elastic constants are performed on solid media. At the surface of the solid a measurement is made of displacement, a vector quantity. The measurement technique is sensitive only to the component of displacement normal to the surface. Thus when the transducers are large enough that the waves can be considered plane, the measured value accurately represents the displacement field, but

when the waves can no longer be considered plane, only the longitudinal component is measured. In contrast, the parameter measured for a fluid medium would be a scalar such as pressure or velocity potential. Thus the fluid theory treats the measurement of a scalar quantity instead of a vector quantity.

The anisotropy of the solid also leads to problems. The wave speed is a function of direction in an anisotropic material, and therefore the assumption of spherical Huyghens' wavelets is not strictly valid. Also, since parts of the diffracted wave travel in nonpure mode directions, there is coupling to transverse modes.

Despite the approximations that must be made to treat the effects of diffraction on the nonlinearity measurements, it has been demonstrated that meaningful measurements can be made using the technique presented. The data obtained in the present experiments are presented as a contribution to the solution of the general problem of the diffraction of waves propagating in a nonlinear medium.

VIII. SUGGESTIONS FOR FURTHER WORK

A result of the present research was to extend the harmonic generation technique for nonlinearity measurements to include measurement of smaller samples than could be measured previously. Consequently, future measurements can include a wider range of materials. The previously existing harmonic generation technique is capable of performing the nonlinearity measurements as a function of temperature down to liquid helium temperature. The temperature dependent measurements can be extended to include small samples by modifying part of the

cryogenic apparatus and utilizing the diffraction correction. This work has been begun by Jacob Philip.

Measurements in the [100] and [110] directions in $KZnF_3$ are reported here. To obtain a third combination of third-order elastic constants a measurement in the [111] direction is needed.

A more rigorous mathematical treatment of the diffraction of finite amplitude waves would be desirable. A tutorial paper by Bajak and Breazeale (1980) presents a quantum mechanical approach to the same problem of plane wave harmonic generation that was treated classically in Chapter II. In the quantum mechanical theory, two phonons of the fundamental frequency interact to produce a phonon of the second harmonic frequency. In the paper there is given an expression for the amplitude of the second harmonic component as a function of the deviation of the direction of the second harmonic wave vector from the direction of the wave vector composed of the sum of the two fundamental frequency wave vectors. This suggests the possibility to correct for diffraction of the second harmonic. A means of implementing the correction for the present experimental configuration would involve resolving the fundamental field into an equivalent set of plane waves and determining the amplitudes of the phonons generated by the many interactions of the phonons in the fundamental field.

LIST OF REFERENCES

LIST OF REFERENCES

Abramowitz, Milton and Irene A. Stegun, eds., Handbook of Mathematical Functions. National Bureau of Standards, 1964.

Bains, J. A., Jr., "Variations of Combinations of Third-Order Elastic Constants in Germanium between 3 and 300°K," Ph.D. dissertation, The University of Tennessee, Knoxville (1974).

Bains, J. A., Jr. and M. A. Breazeale, Phys. Rev. B13, 3623 (1976).

Bajak, I. L. and M. A. Breazeale, J. Acoust. Soc. Am. 68, 1245 (1980).

Barker, L. M. and R. E. Hollenbach, J. Appl. Phys. 41, 4208 (1970).

Bateman, T., W. P. Mason, and H. J. McSkimin, J. Appl. Phys. 32, 928 (1961).

Birch, F., Phys. Rev. 71, 809 (1947).

Bogardus, E. H., J. Appl. Phys. 36, 2504 (1965).

Breazeale, M. A. and J. Ford, J. Appl. Phys. 36, 3486 (1965).

Breazeale, M. A. and D. O. Thompson, Appl. Phys. Lett. 3, 77 (1963).

Brugger, K., Phys. Rev. 133, A1611 (1964).

Cantrell, John H., Jr., "An Ultrasonic Investigation of the Nonlinearity of Fused Silica for Different Hydroxyl Ion Contents and Homogeneities between 300° and 3°K," Ph.D. dissertation, The University of Tennessee, Knoxville (1976).

Cantrell, John H., Jr. and M. A. Breazeale, Phys. Rev. B17, 4864 (1978).

Chang, Z.-P., Phys. Rev. 140, A1788 (1965).

Coldwell-Horsfall, R. A., Phys. Rev. 129, 22 (1963).

Daniels, W. B. and C. S. Smith, Phys. Rev. 111, 713 (1958).

Drabble, J. R. and M. Gluyas, J. Phys. Chem. Solids Supplement 1, 607 (1963).

Dunham, R. W. and H. B. Huntington, Phys. Rev. B2, 1098 (1970).

Fischer, M., A. Zarembowitch, and M. A. Breazeale (to be published in Proceedings of 1980 IEEE Ultrasonics Symposium, 1981).

Fischer, Myriam, "Etude des Constantes Elastiques des $3^{\grave{e}me}$ et $4^{\grave{e}me}$ Orderes de Monocristaux Ioniques," Ph.D. dissertation, Université Pierre et Marie Curie (1979).

Gauster, W. B., "Ultrasonic Measurement of the Non-linearity Parameters of Copper Single Crystals," Ph.D. dissertation, The University of Tennessee, Knoxville (1966); ORNL-TM-1573, 1966.

Gauster, W. B. and M. A. Breazeale, Rev. Sci. Instrum. 37, 1544 (1966).

Gauster, W. B. and M. A. Breazeale, Phys. Rev. 168, 655 (1968).

Gedroits, A. A. and V. A. Krasilnikov, Sov. Phys. JETP 16, 1122 (1963).

Graham, R. A., J. Acoust. Soc. Am. 51, 1576 (1972).

Graham, R. A. and W. P. Brooks, J. Phys. Chem. Solids 32, 2311 (1971).

Hearmon, R. F. S., Acta Cryst. 6, 331 (1953).

Hiki, Y. and A. V. Granato, Phys. Rev. 144, 411 (1966).

Holt, A. C. and J. Ford, J. Appl. Phys. 38, 42 (1967).

Hughes, D. S. and J. L. Kelly, Phys. Rev. 92, 1145 (1953).

Ingenito, F. and A. O. Williams, J. Acoust. Soc. Am. 49, 319 (1971).

Jones, G. L. and D. R. Kobett, J. Acoust. Soc. Am. 35, 5 (1963).

Kunitsyn, V. E. and O. V. Rudenko, Sov. Phys. Acoust. 24, 310 (1978).

Lazarus, D., Phys. Rev. 76, 545 (1949).

Lockwood, J. C., T. G. Muir, and D. T. Blackstock, J. Acoust. Soc. Am. 53, 1148 (1973).

Lommel, E., Abh. Bayer. Akad. Wiss. Math.-Naturwiss. Kl 15, 233 (1886).

Mackey, J. E. and R. T. Arnold, J. Appl. Phys. 40, 4806 (1969).

Mason, Warren P. and R. N. Thurston, eds., Physical Acoustics, Vol. XI, Academic Press, New York, 1975.

McSkimin, H. J. and P. Andreatch, Jr., J. Appl. Phys. 35, 3312 (1964).

Meeks, E. L. and R. T. Arnold, Phys. Rev. B1, 982 (1970).

Melngailis, J., A. A. Maradudin, and A. Seeger, Phys. Rev. 131, 1972 (1963).

Overton, W. C. and J. Gaffney, Phys. Rev. 98, 969 (1955).

Parker, J. H., Jr., E. F. Kelly, and D. I. Bolef, Appl. Phys. Lett. 5, 7 (1964).

Peters, R. D., "Ultrasonic Measurement of the Temperature Dependence of Copper Nonlinearity Parameters," Ph.D. dissertation, The University of Tennessee, 1968; ORNL-TM-2286, 1969.

Peters, R. D., M. A. Breazeale, and V. K. Paré, Rev. Sci. Instrum. 39, 1505 (1968).

Peters, R. D., M. A. Breazeale, and V. K. Paré, Phys. Rev. B1, 3245 (1970).

Pfleiderer, H., Phys. Stat. Sol. 2, 1539 (1962).

Philip, Jacob and M. A. Breazeale (accepted for publication in J. Appl. Phys., 1981, in press).

Rogers, Peter H., "A Theoretical Study of Second-Harmonic Generation in the Acoustic Beam of a Circular Plane Piston," Ph.D. dissertation, Brown University (1970).

Rogers, Peter H. and A. L. Van Buren, J. Acoust. Soc. Am. 55, 724 (1974).

Rollins, F. R., Jr., Appl. Phys. Lett. 2, 147 (1963).

Rollins, F. R., Jr., L. H. Taylor, and P. H. Todd, Jr., Phys. Rev. 136, A597 (1964).

Seeger, A. and O. Buck, Z. Naturforschg. 15a, 1056 (1960).

Seki, H., A. Granato, and R. Truell, J. Acoust. Soc. Am. 28, 230 (1956).

Skove, M. J. and B. E. Powell, J. Appl. Phys. 38, 404 (1967).

Taylor, L. H. and F. R. Rollins, Jr., Phys. Rev. 136, A591 (1964).

Thurston, R. N., H. J. McSkimin, and P. Andreatch, Jr., J. Appl. Phys. 37, 267 (1966).

Thurston, R. N. and M. J. Shapiro, J. Acoust. Soc. Am. 41, 1112 (1967).

Voigt, W., Lehrbuch der Kristallphysik. Teubner, Leipzig und Berlin, 1928.

Yost, W. T., "An Ultrasonic Investigation of the Magnitude and Temperature Dependence of the Nonlinearity Parameters of Germanium and Fused Silica," Ph.D. dissertation, The University of Tennessee, Knoxville (1972).

Yost, W. T. and M. A. Breazeale, J. Appl. Phys. 44, 1909 (1973).

Yost, W. T. and M. A. Breazeale, Phys. Rev. B9, 510 (1974).

Yost, W. T., John H. Cantrell, Jr., and M. A. Breazeale (accepted for publication in J. Appl. Phys., 1980, in press).

APPENDIX

APPENDIX

COMPUTER PROGRAM FOR THE CALCULATION OF THE MAGNITUDE OF

THE DIFFRACTION CORRECTION, $|D_L|$, AS A FUNCTION OF S

The following computer program, DIFCOR.F10, and subroutine,

BES.F10, written in FORTRAN for use on the DECsystem-10 Operating

System, is used to calculate the magnitude of the diffraction

correction, $|D_L|$, as expressed in Eq. (IV.1), as a function of s.

As written, the value of s varies from 0.00 to 74.99 in increments

of 0.01. The program is adapted from that written by D. W. Fitting.

```
00100              REAL J0,J1
00200         .    DIMENSION DIFCOR(7500),RINDEX(750)
00300              DATA PI/3.1415926/
00400              OPEN(UNIT=25,FILE='DIFCOR.OUT',ACCESS='SEQOU
T',
00500         * DEVICE='DSKB:')
00600           DO 10 I=1,7499
00700              S=FLOAT(I)/100.
00800              ARG=2.*PI/S
00900              CALL BES(ARG,J0,J1)
01000         10 DIFCOR(I)= (SQRT((COS(ARG)-J0)**2+(SIN(ARG)-J1
)**2))
01100              DIFCOR(0)=1.0
01200              DO 20 I=1,750
01300         20 RINDEX(I)=FLOAT(I-1)/10.
01400              TYPE 6,(RINDEX(I),(DIFCOR(K),K=(I-1)*10,(I-1
)*10+9),
01500         * I=1,750)
01600         6 FORMAT(1H1/1H0,36X,'DIFFRACTION CORRECTION DL
AS A FUNCTION OF S
01700         * '/1H0,3X,'S',7X,'0.00',6X,'0.01',6X,'0.02',
01800         1 6X,'0.03',6X,'0.04',6X,'0.05',6X,'0.06',6X,
01900         2 '0.07',6X,'0.08',6X,'0.09'/1H0/50(3X,F4.1,10F
10.3/))
02000              END
```

```
00100              SUBROUTINE BES(X,J0,J1)
00200              DIMENSION A(7),B(7),C(7),D(7),E(7),F(7)
00300              REAL J0,J1
00400              DATA A/1.0,-.25,1.562495E-2,-4.34008E-4,6.77
4562E-6,
00500           1 -6.679876E-8,3.95152E-10/,B/.5,-6.249998E-2,2
.604145E-3,
00600           2 -5.424265E-5,6.756882E-7,-5.378753E-9,2.08677
9E-11/,
00700           3 C/7.978846E-1,-2.31E-6,-4.97466E-2,-2.56824E-
3,1.11162E-1,
00800           4 -1.769162E-1,1.0553E-1/,D/-7.853982E-1,-1.249
919E-1,
00900           5 -3.5586E-4,7.089471E-2,-4.384125E-2,-7.127919
E-2,
01000           6 9.883782E-2/,E/7.978846E-1,4.68E-6,1.4937E-1,
4.61835E-3,
01100           7 -2.021039E-1,2.761768E-1,-1.460406E-1/,F/-2.3
56194,
01200           8 3.749884E-1,5.085E-4,-1.722273E-1,6.022188E-2
,1.939723E-1,
01300           9 -2.126201E-1/
01400              IF(X.GT.3.0) GO TO 10
01500              J0=A(1)+X*X*(A(2)+X*X*(A(3)+X*X*(A(4)+X*X*(A
(5)+X*X*(A(6)+
01600           *  X*X*A(7))))))
01700              J1=X*(B(1)+X*X*(B(2)+X*X*(B(3)+X*X*(B(4)+X*X
*(B(5)+X*X*(B(6)+
01800           *  X*X*B(7)))))))
01900              RETURN
02000           10 F0=((((((C(7)/X+C(6))/X+C(5))/X+C(4))/X+C(3))/X
+C(2))/X+C(1)
02100              TH0=((((((D(7)/X+D(6))/X+D(5))/X+D(4))/X+D(3)
)/X+D(2))/X+
02200           *  D(1)+X
02300              F1=((((((E(7)/X+E(6))/X+E(5))/X+E(4))/X+E(3))
/X+E(2))/X+E(1)
02400              TH1=((((((F(7)/X+F(6))/X+F(5))/X+F(4))/X+F(3)
)/X+F(2))/X+
02500           *  F(1)+X
02600              J0=F0*COS(TH0)/SQRT(X)
02700              J1=F1*COS(TH1)/SQRT(X)
02800              RETURN
02900              END
```

REPORTS DISTRIBUTION LIST FOR ONR PHYSICS PROGRAM OFFICE
UNCLASSIFIED CONTRACTS

Director Defense Advanced Research Projects Agency Attn: Technical Library 1400 Wilson Blvd. Arlington, VA 22209	3 copies
Office of Naval Research Physics Program Office (Code 421) 800 North Quincy St. Arlington, VA 22217	3 copies
Office of Naval Research Director, Technology (Code 200) 800 North Quincy St. Arlington, VA 22217	1 copy
Naval Research Laboratories Department of the Navy Attn: Technical Library Washington, DC 20375	3 copies
Office of the Director of Defense Research and Engineering Information Office Library Branch The Pentagon Washington, DC 20301	3 copies
U.S. Army Research Office Box 12211 Research Triangle Park North Carolina 27709	2 copies
Defense Technical Information Center Cameron Station Alexandria, VA 22314	12 copies
Director, National Bureau of Standards Attn: Technical Library Washington, DC 20234	1 copy
Commanding Officer Office of Naval Research Western Regional Office 1030 East Green St. Pasadena, CA 91101	3 copies

Commanding Officer .... 3 copies
Office of Naval Research Eastern/Central Regional Office
666 Summer St.
Boston, MA 02210

Director .... 1 copy
U.S. Army Engineering Research
  and Development Laboratories
Attn: Technical Documents Center
Fort Belvoir, VA 22060

ODDR&E Advisory Group on Electron Devices .... 3 copies
201 Varick St.
New York, NY 10014

Air Force Office of Scientific Research .... 1 copy
Department of the Air Force
Bolling AFB, DC 22209

Air Force Weapons Laboratory .... 1 copy
Technical Library
Kirtland Air Force Base
Albuquerque, NM 87117

Air Force Avionics Laboratory .... 1 copy
Air Force Systems Command
Technical Library
Wright-Patterson Air Force Base
Dayton, OH 45433

Lawrence Livermore Laboratory .... 1 copy
Attn: Dr. W. F. Krupke
University of California
P.O. Box 808
Livermore, CA 94550

Harry Diamond Laboratories .... 1 copy
Technical Library
2800 Powder Mill Rd.
Adelphi, MD 20783

Naval Air Development Center .... 1 copy
Attn: Technical Library
Johnsville
Warminster, PA 18974

Naval Weapons Center .... 1 copy
Technical Library (Code 753)
China Lake, CA 93555

Naval Training Equipment Center   1 copy
Technical Library
Orlando, FL 32813

Naval Underwater Systems Center   1 copy
Technical Center
New London, CT 06320

Commandant of the Marine Corps   1 copy
Scientific Advisor (Code RD-1)
Washington, DC 20380

Naval Ordnance Station   1 copy
Technical Library
Indian _Head, MD 20640

Naval Postgraduate School   1 copy
Technical Library (Code 0212)
Monterey, CA 93940

Naval Missile Center   1 copy
Technical Library (Code 5632.2)
Point Mugu, CA 93010

Naval Ordnance Station   1 copy
Technical Library
Louisville, KY 40214

Commanding Officer   1 copy
Naval Ocean Research & Development Activity
Technical Library
NSTL Station, MI 39529

Naval Explosive Ordnance Disposal Facility   1 copy
Technical Library
Indian Head, MD 20640

Naval Ocean Systems Center   1 copy
Technical Library
San Diego, CA 92152

Naval Surface Weapons Center   1 copy
Technical Library
Silver Springs, MD 20910

Naval Ship Research and Development Center   1 copy
Central Library (Code L42 and L43)
Bethesda, MD 20084

Naval Avionics Facility   1 copy
Technical Library
Indianapolis, IN 46218

Dr. Werner G. Neubauer   1 copy
Code 3180
Physical Acoustics Branch
Naval Research Laboratory
Washington, DC 20375

Dr. Bill D. Cook   1 copy
Dept. of Mechanical Eng.
University of Houston
Houston, TX 77004

Dr. Floyd Dunn   1 copy
Biophysical Research Laboratory
University of Illinois
Urbana, IL 61801

Dr. E. F. Carome   1 copy
Dept. of Physics
John Carroll University
University Heights
Cleveland, OH 44017

Albert Goldstein, Ph.D.   1 copy
Chief, Division of Medical Physics
Henry Ford Hospital
2799 West Grand Blvd.
Detroit, MI 48202